A three-phase reactor assessment for the deployment of Liquid Organic Hydrogen Carriers (LOHCs)

Carlos Prieto[a], Antonio Sánchez[a], Mariano Martín[a,*]

[a]*Department of Chemical Engineering, University of Salamanca, 37008 Salamanca, Spain*

Abstract

As a result of the large increase in the production of renewable energies, energy storage and energy carrier systems are required to meet the most ambitious objectives. In this area, hydrogen stands out as one of the most powerful tools. However, its low volumetric energy density and its challenging storage conditions lead to the search for new forms of storage. Liquid organic hydrogen carriers (LOHCs) are positioned as a promising option to store hydrogen using a catalytic reversible reaction at moderate temperature. Notwithstanding, although reactor technology is the core section of the LOHC process, it has not been assessed yet. Therefore, in this work, a three-phase reactor analysis is performed including mass, heat, and momentum phenomena along with kinetics. In particular, the two most important reactors for three-phase reactions are evaluated, trickle bed and slurry. And two of the most attractive LOHCs systems, dybenzyltoluene and a mixture composed of 1,2-dimethylindole and 7-ethylindole, are considered. The influence of the operating and design variables was studied. The results show that, for hydrogenation slurry reactors, a first region may be formed where gas-liquid is the main resistance (60-95%). It eventually ends up with a second one where kinetics becomes the controlling step. At this point, a better catalyst use is expected for the first region. Alternatively, trickle bed hydrogenation reactors are largely controlled by mass transfer over almost the whole reactor length. If the dehydrogenation process is assessed, kinetics resistance is predominant. Surrogate models are developed to optimize the reactor performance and to include the full reactor operation in futures process design analysis allowing for an effective deployment of LOHCs systems.

Keywords: Hydrogen, Energy storage, Energy carriers, LOHCs, Renewable Energy

*Corresponding author
Email address: mariano.m3@usal.es (Mariano Martín)

1. Introduction

Renewable energy sources (RES) are one of the main instruments to decarbonize the current economic system. During the next years, an unprecedented transformation is expected in the energy sector, including transportation, as it is responsible for around 73% of the global greenhouse gas emissions (GHG) (Ritchie et al., 2020). According to IRENA (2020), global CO_2 emissions should be reduced by around 70% compared to the current levels by 2050 to keep global temperature increase below 2ºC. To meet these demanding requirements, an increase in the share of renewable energies is essential. They should reach up to 66% in terms of final energy consumption and around 90% for electricity production by 2050 (IRENA, 2020). In this new scenario, solar PV and wind energies will be the two predominant energy sources with, for instance, more than 80% of the total power generation (BloombergNEF, 2021). This high penetration of renewable production poses a major challenge due to its fluctuating nature, jeopardizing the equilibrium between supply and demand. In this new green scenario, the use of energy storage technologies becomes essential to ensure the stability and reliability of the electricity grid (Sánchez et al., 2022). Today, a wide range of storage alternatives have been proposed and, according to Gür (2018) they can be classified into four different categories: electrochemical, chemical, mechanical, and thermal. In this broad spectrum, each technology has different properties such as power density, discharge time, round-trip efficiency, or storage horizon. Therefore, depending on the specific application, a suitable solution can be found. For a medium long-term storage horizon, hydrogen emerges as one of the main energy storage alternatives. It allows a wide range of capacities and also avoids storage losses (Colbertaldo et al., 2019) while at the same time is regarded as an effective tool to reduce carbon intensity (Serrano-Arévalo et al., 2023).

In this decarbonzitation scenario, it is necessary not only to focus the attention on the power sector (Meckling et al., 2017). A wider approach is required to decarbonize the transportation, industry, or the heating and cooling sector. All of these fields represent a significant amount of global GHG emissions. In some of them, direct electrification can be a feasible option to replace traditional carbon sources. For example, in the heating and cooling sectors, the introduction of heat pumps is a feasible alternative for some applications. It can replace natural gas-based system using renewables and, according to the analysis proposed by Thomaßen et al. (2021) for the EU countries, the current national power system can address the increase in electricity demand. Another activity where direct electrification is feasible is light-duty vehicles. There, the use of batteries can significantly reduce net emissions even with the current carbon intensity in the power sector (Knobloch et al., 2020). In contrast, others are hard to directly electrify. Some of them are heavy or maritime transport, industrial heating, etc. In order to over-

come related issues to the integration of renewable energies in these essential areas, the use of energy carriers has been widely suggested. Among them, hydrogen stands out for its importance and projection (Hren et al., 2023).

Therefore, green hydrogen is positioned as an essential element for an integral energy transition (Capurso et al., 2022). For a full deployment of the hydrogen economy, two main barriers are identified (Preuster et al., 2017). The first one is related to hydrogen production using a renewable pathway, mainly through water electrolysis. This alternative is currently more expensive than traditional methods based on natural gas reforming. However, ongoing improvements in electrolysis technology (with better efficiency and reduced capital cost) and the reduction in the cost of renewable energy, could make this hydrogen production route competitive in the coming years. The second barrier is the difficult storage and transportation conditions due to its low volumetric energy density and because hydrogen is the lightest element and can leak out of many materials. Currently, different hydrogen storage methods have been investigated such as high-pressure systems, cryogenic storage, or metal hydrides (Niermann et al., 2021). At this point, one of the most interesting and attractive emerging alternatives is the use of liquid organic hydrogen carriers (LOHCs) (Kwak et al., 2021). It allows for simpler hydrogen storage and transport conditions (Narayanan et al., 2022). The idea behind LOHCs is the use of organic chemicals to store hydrogen using a reversible catalytic hydrogenation/dehydrogenation reaction. The main advantages of using LOHCs are the reversibility of the reaction, moderate reaction temperatures, commercial availability of the chemicals proposed as LOHCs, and compatibility with the existing oil infrastructure (He et al., 2015). Nowadays, research is focused on finding the ideal LOHC with good manageability under liquid conditions (avoiding the use of solid or solvents), easy separation from hydrogen, reduced cost, safe, and non-toxic (Rao and Yoon, 2020). Some of the LOHCs that have been proposed are N-ethylcarbazole, dibenzyltoluene, toluene, naphthalene, etc. (Byun et al., 2022).

Research has approached the study of LOHCs deployment from two different perspectives. On the one hand, several authors have investigated the hydrogenation/dehydrogenation reaction of LOHCs from a kinetic point of view. Dong et al. (2019) studied the use of 1,2-dimethylindole as LOHC proposing as catalyst Ru/Al_2O_3 for hydrogenation and Pd/Al_2O_3 for dehydrogenation. Both reactions follow a first order kinetic with a range of temperatures of 130-170ºC for hydrogenation and 170-200ºC for dehydrogenation. Modisha et al. (2019) studied dybenzyltoluene dehydrogenation in a 290-320 ºC range while Jorschick et al. (2017) evaluated both hydrogenation and dehydrogenation using Pt/Al_2O_3 as catalyst for both reactions around 290-310ºC. Following the same approach, Wan et al. (2013) developed a kinetic study of

N-ethylcarbazole as LOHC over Ru/Al_2O_3 using temperatures between 120-160ºC. For this liquid, the reaction follows a first-order kinetics for the concentration of hydrogen and a zero-order for the concentration of N-ethylcarbazole. On the other hand, several research studies have explored the feasibility of using LOHCs at process scale for different real-world applications. Niermann et al. (2019) simulated a global hydrogen ship transport using LOHCs as energy carriers. Their study is focused on three main LOHCs: methanol, dibenzyltoluene, and toluene. From an economic analysis of the global system, methanol shows the highest potential for an effective deployment although all three are technologically mature. For a stationary energy storage system, Eypasch et al. (2017) proposed the use of dibenzyltoluene to address the fluctuations in the power generation from wind turbines and PV panels. With the optimal self-sufficient ratio of 60%, the integrated LOHC system can save around 33% compared to buying electricity from the grid. Byun et al. (2022) evaluated different LOHCs from an economic and an environmental perspective. The strongest economic competitiveness is provided by the dibenzyltoluene system with a unit cost of around 7 $\$/kg$ of H_2. However, the integrative carbon footprint analysis clearly demonstrates the potential environmental advantages of N-ethylcarbazole.

However, between these two perspectives, there is an intermediate step that is required for an effective technology deployment. This refers to an assessment of the hydrogenation/dehydrogenation reactor technology. Notwithstanding, for the design of these reactors, including mass, energy, and momentum balances is essential, apart from kinetics. In particular, this is true for three-phase reactors, which involve a great complexity. Therefore, in this stage, an integral evaluation is performed including, not only, the kinetic rate of the reaction but also the transport phenomena. This analysis is mandatory to be able to calculate the real performance of three-phase LOHC reactors leaving behind the limitations of only a kinetic study. If the limiting step in the reactor system is mass or energy transfer, the use of kinetics cannot capture the full behaviour of the unit. In this situation, the results obtained would not reflect the reality of the system. Thus, with the analysis of the reactor performance, it is possible to obtain accurate results to evaluate, at process scale, the current possibilities of using LOHCs in different energy areas. And, to the best of the authors' knowledge, there is not any other research that addresses this essential issue for the LOHCs system. Particularly, in this work, the two most widespread reactors for solid-liquid-gas reactions have been studied: slurry and trickle bed reactors. For these reactor systems, an integral model is developed including kinetic rate, mass, energy, and momentum transport to capture the behaviour of these complex units. Two of the most promising LOHCs systems involving three-phase systems in hydrogenation and dehydrogenation reactions have been evaluated in

this study: 1) dibenzyltoluene and 2) a mixture of 1,2-dimethylindol and 7-ethylindole. Nevertheless, this rigorous model can be easily extended to all the LOHCs that involve a solid-liquid-gas system.

2. Reactor modelling

The two most important reactor designs are assessed for LOHCs hydrogenation and dehydrogenation reactions: trickle bed and slurry. Detailed 1-dimension models for both are presented below in this section. The benefits of this type of models are found in their lower computational use and simplicity. They are also useful as a first step to further develop more complex models (Manjrekar and Mills, 2022). The scope of this study is to implement a 1-dimension model. It allows to evaluate some of the most relevant variables affecting these systems. This model may eventually be considered for a later construction of more detailed models. For instance, these can be upgraded to rigorous 2 or 3-dimension models (Ekambara et al., 2005).

2.1. Trickle bed reactor model

Trickle beds are well-known reactor units for gas-liquid-solid three-phase reaction applications in the chemical industry. The features of these reactors for hydrogenation purposes makes them suitable to be considered for LOHCs hydrogenation step. Furthermore, trickle beds can also be taken into account for dehydrogenation reactions. It seems advantageous to have a hydrogen gas acceptor to remove it conveniently while is being released during the reaction. Otherwise, its accumulation on pores can lead to undesired hydrogenation. In fact, this practice has been conducted and has evident benefits on conversion (Shen et al., 2014). Moreover, other advantages of introducing gas in trickle bed dehydrogenation reactors are found. These are related to mass transfer enhancement compared to a full liquid situation without gas (Goto and Smith, 1975). To model trickle bed reactors, mass and heat transfer, kinetics and hydrodynamics are evaluated. These are summarized in Figure 1.

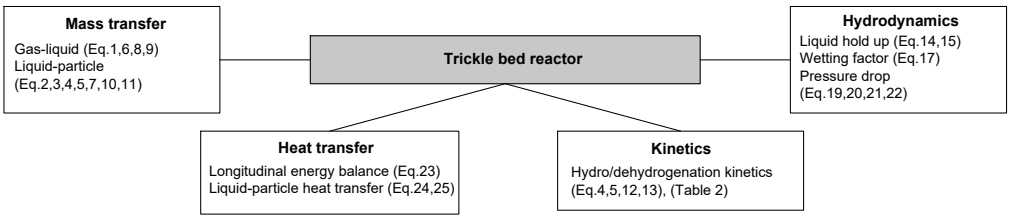

Figure 1: Trickle bed reactor modelling

Trickle bed design consists of a particle catalyst bed where gas and liquid phases flow through voids in a continuous operation mode. Particle size (d_p) may range between 1-5 mm and bed porosities (ϵ) within 0.35-0.40. In general, due to high D_T/d_p relations on industrial units, the wall effect is not relevant (Mederos-Nieto et al., 2020). Catalyst properties from Satterfield et al. (1969) were considered to perform reactor design with spherical particles. These are summarized in Table 1. Except for particle diameter, all catalyst properties will be identical for hydrogenation and dehydrogenation units.

Table 1: Spherical trickle bed catalyst characteristics (Satterfield et al., 1969)

ϵ	0.4	Pore diameter (Å)	75
$dp_{hydro}/dp_{dehydro}$ (mm)	1/3	Catalyst density (kg/m^3)	1620
τ	2.8	Internal porosity	0.498

Relevant design consideration of these units is related to liquid distribution. It plays a major role in the reactor behaviour (Azarpour et al., 2021). Because of that, diameter dimensions are limited to avoid liquid maldistribution up to 3 m (Satterfield, 1975). According to other references, the diameter can be extended up to 4 m and aspect ratios may range from 2.5 to 25 for industrial units (Bhaskar et al., 2004; Jarullah et al., 2012). Co-current downward flow is selected as it is the most extended option (Iliuta and Larachi, 2016). Countercurrent operation is discarded due to higher pressure drops (Mederos-Nieto et al., 2020) and potential flooding (Iliuta and Larachi, 2016; Mederos et al., 2009).

To design trickle bed reactors, a proper selection of trickle bed hydrodynamic regime is required. In general, the most typical ones for these units are trickle and pulsing flow (Manjrekar and Mills, 2022). In this work, the selected regime will be preferably pulsing flow as mass and heat transfer are enhanced when the reactor works on it (Boelhouwer et al., 2001; Westerterp and Wammes, 2000). Medium-high values of gas and liquid flowrates are expected for pulsing flow (Azarpour et al., 2021; Iliuta and Larachi, 2016). For both trickle bed reactors (hydrogenation and dehydrogenation), the liquid flowrate was studied for a range of 1 to 15 kg/m^{2}s. The gas on its side was assessed for a 0.01-0.3 kg/m^{2}s interval. These ranges were selected based on typical operating conditions found in literature (Iliuta and Larachi, 2016; Wang et al., 2013). However, as dehydrogenation units operate near atmospheric conditions, their pressure drop must be minimized. Thus, the lower values for the studied ranges were used for them.

2.1.1. Mass transfer and kinetics

A plug flow model is taken to model gas and liquid phases. Furthermore, it can be considered that both remain at the same temperature during the reaction and that axial dispersion phenomena can be discarded for an industrial unit (Samimi et al., 2015). It is also assumed that gas film resistance will be negligible (Iliuta and Larachi, 2016). This is mainly due to hydrogen low solubility in the liquid phase. Moreover, LOHCs compounds will be supposed not to be transferred to the gas phase as they are considered low-volatility species.

With the previous assumptions, it is possible to formulate the equations that describe mass transfer and chemical reaction. These are referred to all involved reactants: hydrogen and hydrogenated or dehydrogenated LOHCs (depending on hydrogenation/dehydrogenation reaction). Hydrogen transfer from gas-liquid and liquid-to-particle are modelled trough Equation (1) and Equation (2) respectively.

$$\frac{dF_{H_{2,g}}}{dV} = -(k_l a_g)_{H_2}\left(\frac{C_{H_{2,g}}}{H} - C_{H_{2,l}}\right) \tag{1}$$

$$\frac{dF_{H_{2,l}}}{dV} = -(k_m a_m)_{H_2}(C_{H_{2,l}} - C_{H_{2,s}}) \tag{2}$$

In these expressions, F represents molar flow, V the reactor volume, C the concentration in the different phases, and H the hydrogen Henry's coefficient for each LOHCs system. Finally, $k_l a_g$ and $k_m a_m$ refer to volumetric coefficients for gas-liquid and liquid-to-particle mass transfer respectively. Likewise, the mass transfer from the liquid to the particle surface for the LOHCs is represented by Equation (3).

$$\frac{dF_{LOHC_l}}{dV} = -(k_m a_m)_{LOHC}(C_{LOHC_l} - C_{LOHC_s}) \tag{3}$$

Hereinafter, the parallel stage of reaction and catalyst pore diffusion is conducted. Assuming steady state, the mass transfer must equal the reaction rate (r). To refer to each reactant, the mass transfer is divided by its stoichiometric coefficient (v_i). The reaction rate can be characterized by the reaction rate on the catalyst surface (r_s) corrected with the effectiveness factor (η). The equations that model this stage with regards to hydrogen and LOHCs are Equation (4) and Equation (5) respectively.

$$\frac{(k_m a_m)_{H_2}(C_{H_{2,l}} - C_{H_{2,s}})}{v_{H_2}} = \eta r_s \tag{4}$$

$$\frac{(k_m a_m)_{LOHC}(C_{LOHC_l} - C_{LOHC_s})}{v_{LOHC}} = \eta r_s \tag{5}$$

To estimate the mass transfer coefficients, Goto and Smith (1975) experimental data, correlated and tested by Roininen et al. (2009), were considered for this model. Hence, gas-liquid and liquid-to-particle coefficients are obtained from Equation (6) and Equation (7) respectively. There, some liquid properties as density (ρ), viscosity (μ) and diffusion coefficient (D) with some operating variables such as liquid flow rates (L) are required.

$$\frac{(k_l a_g)_i}{(D_i)} = 10^4 \alpha_l \left(\frac{10^{-2} L}{\mu_l}\right)^{n_l} \left(\frac{\mu_l}{D_l \rho_l}\right)^{0.5} \tag{6}$$

$$\frac{(k_m a_m)_i}{(D_i)} = 10^4 \alpha_s \left(\frac{10^{-2} L}{\mu_l}\right)^{n_s} \left(\frac{\mu_l}{D_l \rho_l}\right)^{1/3} \tag{7}$$

The parameters α_l and n_l required to compute gas-liquid transfer are calculated as follow:

$$\alpha_l = a d_p + b \qquad \begin{array}{llll} d_p > 0.0291\ m & a = -2623 & b = 13.63 \\ d_p < 0.0291\ m & a = -759.8 & b = 8.211 \end{array} \tag{8}$$

$$n_l = c d_p + e \qquad \begin{array}{llll} d_p > 0.0291\ m & c = -8.197 & d = 0.4339 \\ d_p < 0.0291\ m & c = 8.442 & d = 0.3854 \end{array} \tag{9}$$

Their respective counterparts, α_s and n_s, for the liquid-to-particle mass transfer are calculated by equations (10) and (11).

$$\alpha_s = -57780 d_p + 184.3 \tag{10}$$

$$n_s = -58.86 d_p + 0.7018 \tag{11}$$

The calculation of the effectiveness factor can be performed with Equation (12) for a spherical particle.

$$\eta = \frac{1}{\phi}\left(\frac{1}{tanh(3\phi)} - \frac{1}{3\phi}\right) \tag{12}$$

Table 2: LOHCs kinetics

	Intrinsic kinetics ($kmol_{LOHC}/s \cdot kg_{cat}$)	Source
Dibenzyltoluene hydrogenation	$1.66 \cdot e^{\frac{-40kJ/mol}{RT}} \cdot C_{DBT}$	(Jorschick et al., 2017; Shi et al., 2020)
Dibenzyltoluene dehydrogenation	$1.47 \cdot 10^{12} \cdot e^{\frac{-205kJ/mol}{RT}} \cdot C_{PHDBT}$	(Modisha et al., 2019)
1,2-dimethylindole hydrogenation	$1.30 \cdot 10^{7} \cdot e^{\frac{-85.1kJ/mol}{RT}} \cdot C_{1,2-DMI}$	(Dong et al., 2019)
1,2-dimethylindole dehydrogenation	$1.05 \cdot 10^{8} \cdot e^{\frac{-111.9kJ/mol}{RT}} \cdot C_{PH-1,2-DMI}$	(Dong et al., 2019)
7-ethylindole hydrogenation	$190 \cdot e^{\frac{-51.5kJ/mol}{RT}} \cdot C_{7-EI}$	(Chen et al., 2018)
7-ethylindole dehydrogenation	$2.03 \cdot 10^{6} \cdot e^{\frac{-101.9kJ/mol}{RT}} \cdot C_{PH-7-EI}$	(Chen et al., 2018)

It is obtained from the Thiele modulus (ϕ), defined in Equation (13) for an nth reaction order (Ross, 2019).

$$\phi = \frac{6}{d_p}\sqrt{\frac{kC_s^{n-1}}{2D_{eff}}} \tag{13}$$

In this equation, D_{eff} and k represent the effective diffusion coefficient and the reaction kinetic constant.

Finally, dybenzyltoluene hydrogenation (Jorschick et al., 2017; Shi et al., 2020) and dehydrogenation kinetics (Modisha et al., 2019) are included in the model. Similarly, they are introduced for 1,2-dimethylindole (Dong et al., 2019) and 7-ethylindole hydrogenation and dehydrogenation (Chen et al., 2018). The presence of LOHCs hydrogenated intermediate species has not been considered since high selectivities are reported (Dong et al., 2019). The used hydrogenation and dehydrogenation kinetics are included in Table 2.

It must be noticed that, for dehydrogenation reactors, the hydrogenated LOHC will be the only reactant. Nevertheless, two species react during hydrogenation: hydrogen and dehydrogenated LOHC. It must be assured for the reaction to occur, that both are able to be fully transferred to the catalyst active center. Otherwise, the reaction can not be carried out regardless of other reactive having high kinetic or/and mass transfer rates. Then, combined mass transfer with kinetics is calculated for each reactant and finally, the slowest reaction rate is taken as the overall one for the stationary scenario. If not, reactor performance may be overestimated as higher rates may be used without considering relevant mass transfer for all reacting species.

2.1.2. Hydrodynamics: liquid holdup, particle wetting and pressure drop

Liquid holdup and particle wetting are relevant parameters when trickle bed reactors are designed. The liquid holdup will have a large influence on the mass and heat transfer but also to avoid hot spots or reactor runaway (Iliuta and Larachi, 2016). Hold-

up can be divided into external and internal. External is sub-divided into a second classification: static (ϵ_{static}) and dynamic ($\epsilon_{dynamic}$). While dynamic represents the liquid fraction that is in continuous movement, static hold-up accounts for the stagnant liquid zones near particles (Manjrekar and Mills, 2022). The static hold-up is calculated through Equation (14) with σ being the surface tension (Sáez and Carbonell, 1985).

$$\epsilon_{static} = \frac{1}{20 + 0.9\left(\frac{\rho_l g d_p^2 \epsilon^2}{\sigma_l (1-\epsilon)^2}\right)} \tag{14}$$

Then, dynamic hold-up can be estimated with Equation (15) (Ellman et al., 1990),

$$\epsilon_{dynamic} = 10^{\left(0.001 - \frac{0.16}{\left(\left(\frac{\rho_l}{\rho_g}\right)^{0.25}\left(\frac{L}{G}\right)^{0.5} Re_l^{-0.25} We_l^{0.2}\left(6\left(\frac{16\epsilon^3}{9\pi(1-\epsilon)^2}\right)^{0.33}\right)^{0.25}\right)^{0.65}}\right)} \tag{15}$$

where G is the gas flowrate and We is Weber adimensional number defined in Equation (16) .

$$We_l = \frac{L^2 d_p}{\rho_l \sigma_l} \tag{16}$$

Finally, related to the internal hold-up, if catalyst pores are completely filled with liquid, its value can be assumed to be equal to ϵ_{in} (Mederos-Nieto et al., 2020).

The wetting factor (w_f) refers to the fraction of catalyst particles wetted by the liquid phase. It is used as a measure of the actual catalyst use (Samimi et al., 2015). Higher wetting factors are required on this model to avoid reaction slow down or hot spots (Westerterp and Wammes, 2000). The hot spots formation causes catalyst deactivation or/and lower selectivities. In general, these are minimized when the operation moves to pulsing region (Boelhouwer et al., 2001), which is the selected regime. To estimate the wetting factor, Equation (17) is applied (Mills and Dudukovic, 1981).

$$w_f = 1 - e^{-1.35 Re_l^{0.333} Fr_l^{0.235}\left(\frac{L^2}{\sigma_l \rho_l a_m}\right)^{-0.170}\left(\frac{6(1-\epsilon)}{\epsilon^2}\right)^{-0.0425}} \tag{17}$$

In this expression, Fr is the Froude number defined in Equation (18) and a_m is the bed specific area.

$$Fr_l = \frac{a_m L^2}{\rho_l^2 g} \tag{18}$$

To estimate two phase-flow pressure drop ΔP_{LG}, Equation (19) is used (Satterfield,

1975).

$$log_{10}\left(\frac{\Delta P_{lg}}{\Delta P_l + \Delta P_g}\right) = \frac{0.416}{(log_{10}(\chi))^2 + 0.666} \tag{19}$$

In this equation, ΔP_G and ΔP_L represent gas and liquid flowing independently pressure drop respectively, whereas χ parameter is defined in Equation (20).

$$\chi = \left(\frac{\Delta P_l}{\Delta P_g}\right)^{0.5} \tag{20}$$

To account for independent gas and liquid pressure drops, Equations (21) and (22) are applied, where u' is the linear velocity (Ergun, 1952).

$$\Delta P_g = \left(\frac{150\mu_g u_g^{'}(1-\epsilon)^2}{d_p^2\epsilon^3}\right) + \left(\frac{1.75\rho_g u_g^{'2}(1-\epsilon)}{d_p\epsilon^3}\right) \tag{21}$$

$$\Delta P_l = \left(\frac{150\mu_l u_l^{'}(1-\epsilon)^2}{d_p^2\epsilon^3}\right) + \left(\frac{1.75\rho_l u_l^{'2}(1-\epsilon)}{d_p\epsilon^3}\right) \tag{22}$$

2.1.3. Heat transfer

Heat transfer limitations is one of the bottlenecks of this reactor design (Boelhouwer et al., 2001). As a result, industrial units typically operate under adiabatical conditions (Azarpour et al., 2021; Samimi et al., 2015). Thus, this operation regime is selected for the model. It is assumed that temperature radial gradient can be discarded for a plug flow behaviour. However, other generated temperature differences must be accounted for: longitudinal, interparticular and intraparticular. Due to the reaction, temperature increases in hydrogenation (exothermic) or decreases in dehydrogenation (endothermic) over the reactor length. To study its profile with reactor volume, an energy balance to a differential element is presented in Equation (23) with T_l, ΔH_r and Cp_i being bulk liquid temperature, reaction enthalpy and specific heat for each specie respectively.

$$\frac{dT_l}{dV} = \frac{r(-\Delta H_r)}{\sum_i F_i Cp_i} \tag{23}$$

Interparticular temperature gradient studies are also required to avoid undesired hot spots. To assess it, Equation (24) is included. There, T_s is the surface temperature.

$$h_{l-s}a_m(T_s - T_l) = r(-\Delta H_r) \tag{24}$$

The convection heat transfer coefficient (h_{l-s}) between the bulk liquid and the catalyst surface is calculated from Equation (25) based on Boelhouwer et al. (2001).

$$\frac{hd_h}{\rho_l} = 0.111 Re_l^{0.8} Pr^{0.33} \tag{25}$$

Where, Pr and d_h represent the Prandtl adimensional number and the hydraulic diameter respectively. Finally, intraparticular gradients are neglected due to liquid filling catalyst pores (Mederos-Nieto et al., 2020).

2.2. Slurry reactor model

Slurry reactors are based on a liquid phase holding suspended solid catalyst particles by the action of a gas introduced at the bottom of the column. For moderate catalyst concentrations, a solid-liquid pseudophase known as slurry where particles are homogeneously distributed can be assumed (Forret et al., 2006). Then, fed gas is dispersed into fine bubbles using a gas sparger. The aim is to maximize gas-liquid mass transfer (Zehner and Kraume, 2000). The operating regime is selected to be continuous (Mederos et al., 2009).

Some examples of slurry hydrogenation reactors have been found in literature for similar liquid systems such as benzene (Zehner and Kraume, 2000). Thus, slurry reactors seem suitable for the studied LOHCs hydrogenation. With regards to LOHCs dehydrogenation, it may be carried out on these units too. This reaction is characterized to have high-demanding temperature conditions (Niermann et al., 2019) at the same time that intrinsic endothermicty reduces the temperature. Therefore, the slurry reactor design could be used to perform an isothermal reaction, taking thus advantage of its proper temperature control. In addition, introducing hydrogen in spite of being a reaction product will be beneficial as it can act as a gas acceptor (Shen et al., 2014). Other benefits are also found as it will enhance mass and heat transfer and provide the required energy for catalyst suspension. The slurry model includes mass and heat transfer, hydrodynamics, gas sparger design and kinetics. These areas are summarized in the Figure 2.

The particle sizes for slurry reactors are considerably lower than for trickle bed reactors ones. Typical porous 50 μm size particles are considered (Biardi and Baldi, 1999). The main benefit of using lower sizes is a considerable reduction in external mass transfer resistance (Dorostkar et al., 2021). Notwithstanding, it brings a major drawback to particle separation systems. Thus, slurry reactor bottlenecks are found on catalyst recovery, lines plugging, and possible losses due to particle abrasion (Mederos et al., 2009). The properties of the catalyst used are summarized in Table 3.

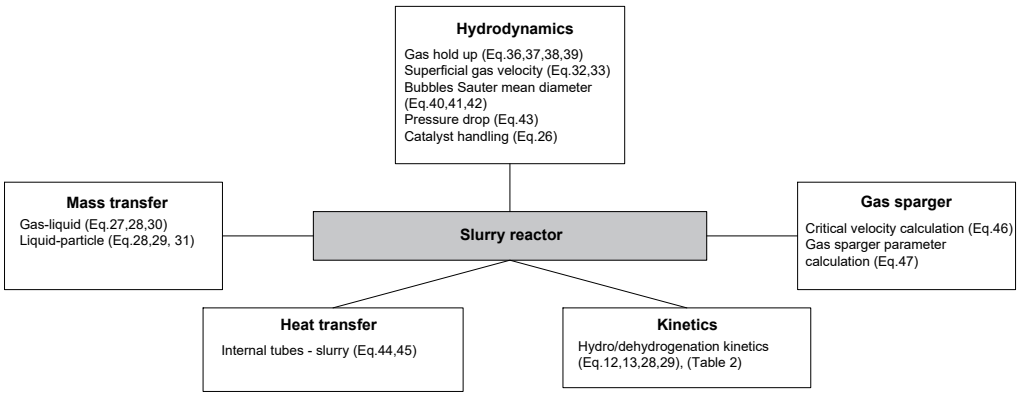

Figure 2: Slurry reactor modelling

Table 3: Spherical slurry catalyst characteristics (Kenney and Sedriks, 1972; Biardi and Baldi, 1999)

Internal porosity	0.54	Pore diameter (Å)	53.2
d_p (μm)	50	Catalyst density (kg/m^3)	1525
τ	1.6		

These catalyst particles can be suspended and therefore used to favor reaction progress thanks to sparged gas action. Thus, to calculate minimum superficial gas velocity ($u_{g,min}$) to suspend a certain catalyst concentration (C_s) on these units, Equation (26) can be used (Zehner and Kraume, 2000).

$$\frac{u_{g,min}}{v_s} = 0.801 \left(\frac{\rho_s - \rho_l}{\rho_l}\right)^{0.600} \left(\frac{C_s}{\rho_s}\right)^{0.146} \left(\frac{\sqrt{gD_T}}{v_s}\right)^{0.240} \left(1 + 807 \left(\frac{g\mu_l^4}{\rho_l \sigma_l^3}\right)^{0.578}\right) \quad (26)$$

On this expression, v_s represents the settling velocity for the particles and D_T the reactor diameter. Likewise trickle bed, slurry reactors are also characterized by having different operating regimes (homogeneous, slug flow and churn-turbulent or heterogeneous). Industrial columns tend to operate under churn-turbulent regime. Hence, it is selected for the proposed reactor design (Wang et al., 2007) because mass and heat transfer are favored (Forret et al., 2006). A minimum 0.15 m column diameter is required for this regime (Besagni et al., 2019) together with superficial gas velocities starting from 0.08 m/s (Zehner and Kraume, 2000). Then, typical diameter sizes ranging from 0.5 to 4 m are considered for the current design according to literature values. Moreover, aspect ratio is set between 4 and 20 (Behkish et al., 2006).

2.2.1. Mass transfer and kinetics

To characterize these units, a perfect mixture model is assumed for the slurry phase (Mamabolo and Nkazi, 2019). A hybrid approach is used to model the gas phase considering a bi-modal dispersion. Two bubble sizes are taken: small and large. Small ones can be described with a perfect mixture model as they will be homogeneously distributed. On the contrary, large bubbles will travel along column height with a plug-flow behaviour (Maretto and Krishna, 1999). Steady state is assumed and gas film transfer resistance is neglected (Mamabolo and Nkazi, 2019). Thus, to describe hydrogen mass transfer and kinetics, Equations (27) and (28) are used.

$$\frac{dF_{H_{2,g}}}{dV_{sl}} = -(k_l a_g)_{H_2}\left(\frac{C_{H_{2,g}}}{H} - C_{H_{2,l}}\right) \tag{27}$$

$$\frac{(k_l a_g)_{H_2}\left(\frac{C_{H_{2,g}}}{H} - C_{H_{2,l}}\right)}{v_{H_2}} = \frac{(k_m a_m)_{H_2}(C_{H_{2,l}} - C_{H_{2,s}})}{v_{H_2}} = \eta r_s \tag{28}$$

The mass transfer and reaction over the catalyst for the LOHCs will be modeled by Equation (29). The kinetics referred to intrinsic reaction rate are included in Table 2. Furthermore, it is also assumed that the slowest reactant velocity is the limiting rate and it is used for the design of the unit.

$$\frac{(k_m a_m)_{LOHC}(C_{LOHC_l} - C_{LOHC_s})}{v_{LOHC}} = \eta r_s \tag{29}$$

To estimate the gas-liquid mass transfer coefficient for small and large bubble sizes, the expression proposed by Lemoine et al. (2008) is used and included in Equation 30. For both sizes, the gas hold-up (ϵ_g) and the Sauter mean diameter (d_{Sauter}) are required.

$$k_l a_{g,jB} = 6.14 \cdot 10^4 \left(\frac{\rho_l^{0.26}\mu_l^{0.12}\epsilon_{g,jB}^{1.21}D_l^{0.50}}{\sigma_l^{0.52}\rho_g^{0.06}u_{g,jB}^{0.12}d_{Sauter,jB}^{0.05}T_{sl}^{0.68}}\right)\Gamma^{0.11}\left(\frac{D_T}{D_T+1}\right)^{0.40} \tag{30}$$

The liquid-to-particle mass transfer coefficient is obtained from Ramachandran and Chaudhari (1983) (presented in Equation (31)).

$$\frac{k_{m,i}d_p}{D_i} = 2 + 0.212\left(\frac{d_p^3(\rho_s - \rho_l)g}{\mu_l D_i}\right)^{0.33}\left(\frac{d_p u_g \rho_l}{\mu_l}\right)^{0.112} \tag{31}$$

2.2.2. Hydrodynamics: gas hold-up, superficial gas velocity, Sauter mean diameter and pressure drop

To characterize system hydrodynamics, the superficial gas velocities for small ($u_{g,SB}$) and large sizes ($u_{g,LB}$) are demanded. The relation between both and the global velocity (u_g) is given by Equation (32) (Krishna and Ellenberger, 1996).

$$u_{g,LB} = u_g - u_{g,SB} \tag{32}$$

The superficial velocity of the small bubbles is assumed to be equal to the transition point from homogeneous to the heterogeneous regime. Thus, equation (33) is used to determine the superficial gas velocity value for that situation (Reilly et al., 1994).

$$u_{g,SB} = V_{g,SB}\epsilon_{trans}(1 - \epsilon_{trans}) \tag{33}$$

To compute the small bubbles rise velocity ($V_{g,SB}$), Equation (34) is used for no solids condition (V_{g,SB_0}) (Reilly et al., 1994) and corrected with Equation (35) to include the effect of the solids (Maretto and Krishna, 1999).

$$V_{g,SB_0} = \frac{\sigma_l^{0.12}}{2.84\rho_g^{0.04}} \tag{34}$$

$$V_{g,SB} = V_{g,SB_0}\left(1 + \frac{0.8\epsilon_s}{V_{g,SB_0}}\right) \tag{35}$$

In the same way, hold-up for the transition point without solids ($\epsilon_{g,trans_0}$) is calculated through equation (36) (Reilly et al., 1994) and corrected with expression (37) to account for the presence of the solids ($\epsilon_{g,trans}$) (Maretto and Krishna, 1999).

$$\epsilon_{g,trans_0} = 4.46\sqrt{\frac{\rho_g^{0.96}\sigma_l^{0.12}}{\rho_l}} \tag{36}$$

$$\epsilon_{g,trans} = \epsilon_{g,trans_0}\left(1 - \frac{0.7C_s}{\epsilon_{g,trans_0}}\right)\left(\frac{\rho_g}{\rho_{g,ref}}\right)^{0.48} \tag{37}$$

Large and small bubble hold-ups are obtained from equations (38) and (39) (Krishna

and Ellenberger, 1996).

$$\epsilon_{g,LB} = 0.268\left(\frac{(u_g - u_{g,SB})^{0.58}}{D_T^{0.18}}\right) \tag{38}$$

$$\epsilon_{g,SB} = \epsilon_{g,trans}(1 - \epsilon_{g,LB}) \tag{39}$$

The bimodal dispersion is represented by the Sauter mean diameter of the small and large bubble sizes. They are estimated from the expressions proposed by Lemoine et al. (2008), and these are included in equations (40),(41), and (42).

$$d_{Sauter} = 37.19u_g^{0.14}\left(\frac{\mu_l^{0.08}\sigma_l^{1.22}\rho_g^{0.02}T_{sl}^{1.66}}{\rho_l^{1.52}MW_g^{0.12}}\right)\left(\frac{D_T}{D_T+1}\right)^{0.3} (1-\epsilon_g)^{1.56}\Gamma^{-0.02}e^{-2.29X_w+2.81C_{s,v}+2.77\rho_s d_p} \tag{40}$$

$$d_{Sauter,LB} = d_{Sauter}^{0.96}(1 - 10^{-5}\rho_l^{0.22}\mu_l^{0.03}\sigma_l^{8.60}u_g^{0.04}\epsilon_g^{2.37}\epsilon_{g,LB}^{2.74}) \tag{41}$$

$$\frac{\epsilon_{g,SB}}{d_{Sauter,SB}} = \frac{\epsilon_g}{d_{Sauter}} - \frac{\epsilon_{g,LB}}{d_{Sauter,LB}} \tag{42}$$

Compared to trickle bed reactors, the slurry design will present lower pressure losses (Forret et al., 2006). To estimate pressure drop, Equation (43) can be applied (Sehabiague et al., 2008).

$$\frac{dP}{dz} = -g((1-\epsilon_g)\rho_{sl} + \epsilon_g\rho_g) \tag{43}$$

2.2.3. Heat transfer

Slurry reactors are popular because they provide adequate temperature control (Biardi and Baldi, 1999; Lemoine et al., 2008) and proper heat transfer (Buwa et al., 2016). This is mainly due to the perfect mixture behaviour, which reduces temperature gradients. They present also high heat transfer coefficients for the slurry side (h_{sl}) (Maretto and Krishna, 1999). These features make possible to assume isothermicity in the slurry phase (Mamabolo and Nkazi, 2019; Maretto and Krishna, 1999). Moreover, temperature gradients between the liquid and solid phases are discarded (Mamabolo and Nkazi, 2019).

The intrinsic exo- and endothermicity associated with hydrogenation and dehydrogenation reactions requires cooling and heating respectively. Boiling water is used for

cooling purposes. For heating, high-pressure steam and hot oil are used for indoles and dybenzyltoluene systems respectively. Heat transfer coefficients for these utilities are estimated from Sinnott and Towler (2020a). Furthermore, typical fouling factors and pipe material conductivity are used from the same reference. Referred to the slurry side coefficient, it is estimated from the correlation proposed by Sehabiague et al. (2008), given by Equation (44).

$$h_{sl} = 11710 u_g^{0.445} (\mu_{SL} \cdot 10^3)^{-0.060} (P \cdot 0.1)^{0.176} \tag{44}$$

Then, the required heat transfer areas (A) for both reactions types can be calculated using Equation (45) based on temperature difference (ΔT), overall heat transfer coefficient (U), reaction rate, and its associated enthalpy (ΔH_r).

$$(-\Delta H_r) r = U A \Delta T \tag{45}$$

These heating or cooling demands will be supplied by internal tubes. However, these must not surpass 20% of the volume reactor. This is done to not limit reactor hydrodynamics and mass transfer (Sehabiague et al., 2008).

2.2.4. Gas sparger design

The gas is dispersed to form small bubbles using a gas sparger. Several designs are available (Zehner and Kraume, 2000). However, pipe spargers are the most common when column diameters exceed 1 m (Kulkarni and Joshi, 2011). Hence, typical spider ring design is the selected one. The hole diameter is set to 5 mm diameter size surpassing the minimum 1-2 mm size according to Besagni et al. (2019).

To calculate the number of orifices of the sparger, undesired weeping phenomena are considered. Gas hole velocity must exceed the critical weep velocity value. This limiting point is calculated with Equation (46) (Kulkarni and Joshi, 2011) and then, a 25% security factor is included to design the final slurry sparger.

$$u_{weep} = \sqrt{\left(\frac{0.44(\rho_l - \rho_g d_o g)}{\rho_g}\right)\left(\frac{L_{pipe}}{d_o}\right)^{-0.12}\left(\frac{H_l}{d_o}\right)^{0.67}\left(\frac{L_o}{d_o}\right)^{-0.145}} \tag{46}$$

In this equation, L_{pipe} represents pipe length, H_l static liquid head, d_o is the gas sparger hole diameter and L_o the distance from two adjacent sparger holes.

Finally, the gas sparger parameter (Γ) is also required as its influence is introduced in the previous expressions. It can be calculated based on Equation (47) from Behkish

et al. (2006).

$$\Gamma = (Kd \cdot N_o d_o^{\alpha_{gs}}) \tag{47}$$

There, Kd and α_{gs} represent characteristic gas sparger constants. These are available for several designs. For a spider gas-sparger, selected in this work, these constants are 1 and 0.015 respectively (Behkish et al., 2006).

3. Results

With the models proposed above it is possible to evaluate the influence of operational and design parameters on the behaviour of the reactors. Therefore, both slurry and trickle bed designs are assessed for hydrogenation and dehydrogenation purposes.

3.1. LOHCs hydrogenation

First, hydrogenation slurry reactors are analyzed. Dibenzyltoluene hydrogenation conversion is represented against normalized volume in Figure 3 for different operating conditions. Particularly, temperature, pressure, and the excess of hydrogen are studied. As can be seen, two well-differentiated zones are found. In the first one, the conversion shows a marked positive influence with the excess of H_2 and its pressure. In this region the gas-liquid hydrogen transfer is the limiting step. Then, H_2 excess (gas velocities) and pressure (both beneficial to mass transfer) seem to have negligible effect in a second region. This occurs as the mass transfer begins to lose its importance in favor of the kinetics caused by the reduction in the concentration of LOHCs. Thus, conversions converge for all superficial gas velocity and pressure cases, although temperature continues to be beneficial as it enhances kinetics.

Referring to the first zone, controlled by the gas-liquid mass transfer, an increase in temperature, pressure and gas velocities is advantageous. Their benefits in conversion are due to different reasons. Higher hydrogen solubilities are expected in the proposed LOHCs systems at higher pressures and temperatures. Thus, both will improve hydrogen mass transfer to the liquid phase. In addition, increasing superficial gas velocities favors hydrogen transfer due to the enhancenment of mass transfer coefficients as higher turbulence is produced. The extent of the first region depends on the operating conditions. As high pressures and gas velocities will favor mass transfer, both limit this region extent to lower conversion values. This is because intrinsic kinetic resistance will be predominant over mass transfer earlier. In contrast, although high temperatures also have a positive impact on mass transfer, they will be largely more beneficial to kinetics.

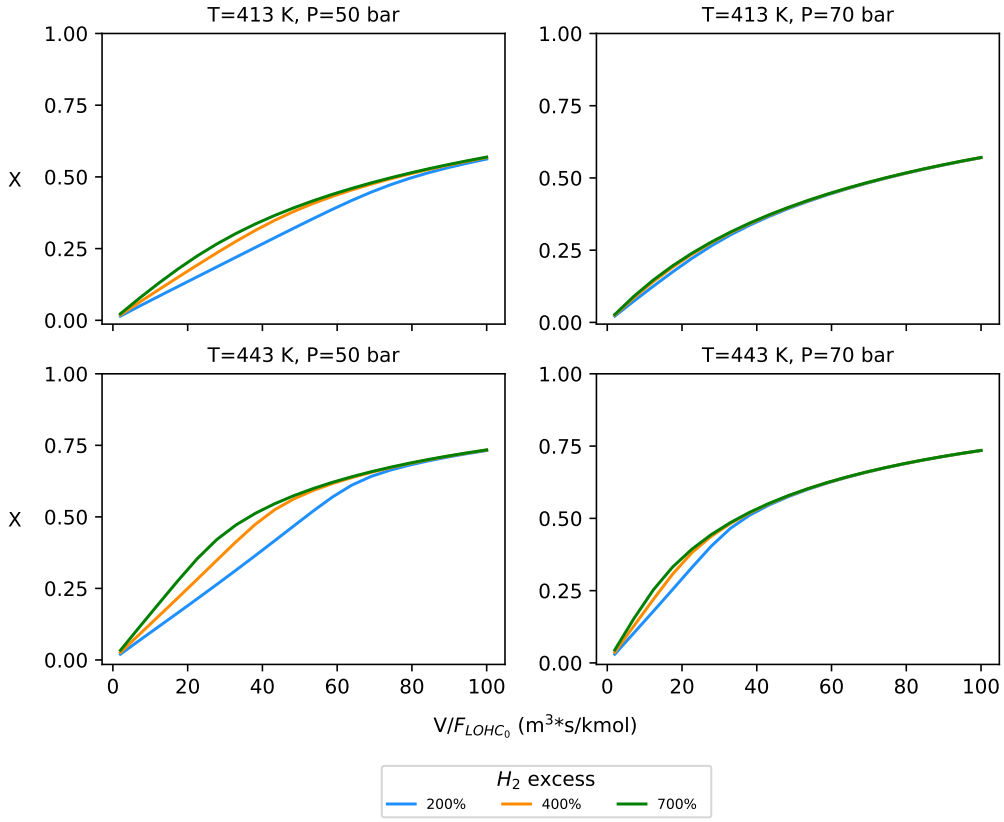

Figure 3: Dibenzyltoluene hydrogenation conversion in slurry reactor for different operating conditions. Dibenzyltoluene pure feed, C_s= 300 kg/m^3

For that reason, when operating at higher temperatures, the mass transfer controlling region will end up at higher conversions.

The change in the limiting rate for the reactors from a mass transfer controlling zone to a second one where they are kinetic-controlled can be analyzed based on reaction resistance distribution depicted in Figure 4. Initially, gas-liquid mass transfer represents about 70-95% of total resistance, showing the predominance of mass transfer phenomena. However, when the transition between regions is reached, kinetics start to have a larger contribution. At this point, gas-liquid resistance is reduced partially. This is due to the fact that the overall rate, including mass transfer and kinetics, for the hydrogen is still lower than the one of the LOHCs. However, if hydrogen transfered faster, the gas-liquid resistance can be neglected as more hydrogen than required would reach the liquid phase. In this situation, the LOHCs would end up becoming the reactant that controls the reaction progress. Hence, as long as they are only transferred from the liquid to

particles, gas-liquid resistance virtually dissapears. When this happens, the second region (having a lesser influence by gas-liquid) may lead to a third region where kinetics will become the limiting step and gas-liquid resistance no longer exists. This will only occur at higher conversions than presented in Figure (3). With regards to the evolution of other resistance contributors, kinetics is close to zero at the beginning. However, as the reaction progress, it will start to gradually grow until it reaches almost 100% contribution for higher conversions than presented. Finally, liquid-to-particle mass transfer decreases as the reaction progress from a maximum of 10% to almost zero.

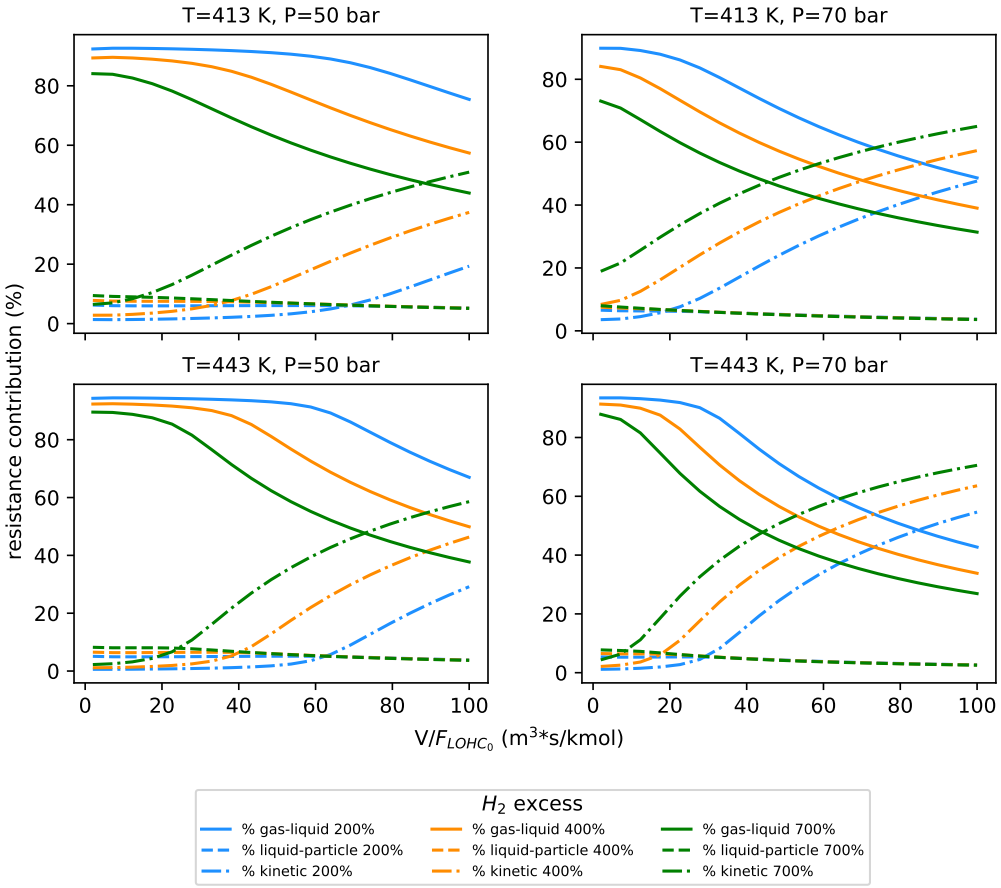

Figure 4: Dibenzyltoluene hydrogenation reaction resistances in slurry reactor for different operating conditions. Dibenzyltoluene pure feed, C_s= 300 kg/m^3

Similar behaviour is found for 1,2-dimethyhlindole and 7-ethylindole hydrogenation when working at the same operating conditions. A first zone is formed where gas-liquid is the main resistance (60-90%), followed by the previously described sec-

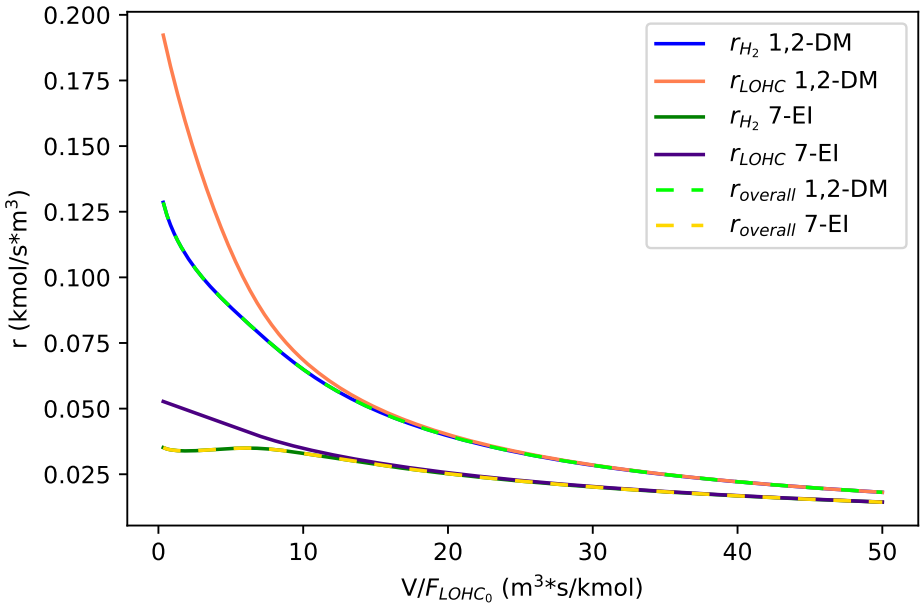

Figure 5: 1,2-dimethylindole (r1,2-DM) and 7-ethylindole (r7-EI) global hydrogenation reaction velocities with its respective hydrogen (rH_2 1,2-DM and rH_2 7-EI) and LOHC (rLOHC 1,2-DM and rLOHC 7-EI) velocities in slurry reactor. 1:1 molar relation 1,2-dimethylindole: 7-ethylindole, C_s= 300 kg/m^3, T= 413 K, P= 70 bar

ond region. In Figure 5, the overall reaction velocity for 1,2-dimethylindole and 7-ethylindole systems are represented against normalized volume. In the same representation, global velocities referred to each of the reactives (hydrogen and LOHCs) are also included. It is shown how the combined rate of mass transfer and kinetics for the hydrogen is initially lower than the one for LOHCs. It results in the overall reaction rate being equal to the rate referred to hydrogen. Beyond this point, overall rates for LOHCs and hydrogen tend to be almost equal. This occurs when the transition point has been reached and kinetics becomes the main resistance. The transition between regions is found for the two indoles hydrogenation reactions at 70-95% and 40-70% conversions for 1,2-dimethylindole and 7-ethylindole respectively. With regards to previous dybenzyltoluene hydrogenation, this point is reached at conversions up to 70%. The higher conversions for 1,2-dimethylindole are mainly attributted to faster kinetics compared to the other LOHCs. It must be noticed that, if catalyst loads are reduced in both systems, kinetic resistance will increase, and then, only one region may be formed. In this situation, kinetics limits the overall reaction rate. This is more likely for the lower operating temperatures and higher pressures as gas-liquid resistance can be neglected if

compared to the kinetics. Similar patterns are identified for the situation in which the reaction is controlled by kinetics over the whole range of volumes. Two marked tendencies are found: a first one with higher slopes to end up with a second one where conversion shows an asymptotic behaviour. This is caused by the larger impact of the concentration of LOHCs on the reaction rate at higher conversions.

The fact that both slurry reactors show two marked tendencies, independently of whether they are mass and kinetic controlled or only kinetic controlled, poses the question on which the reactor should be designed. Figure 3 shows steeper slopes for the first region compared to the second one: at least 2 times larger for dybenzyltolune and 5 and 3 for 1,2-dimethylindole and 7-ethylindole respectively. These results reflect that more efficient catalyst use is found in the first zone when reactor volumes are lower. It indicates the benefits to design a reactor in the gas-liquid controlling region or in the first reaction stages (if it is completely kinetic controlled). These results make sense as perfect mixture designs usually reach medium-higher conversions to avoid lower reactants concentration. Otherwise, kinetics would be largely controlling with excessive unit oversizing. Moreover, it is shown that higher conversions are expected when reactors are controlled only by kinetics. At this point, variables such as temperature and the quantity of catalyst used would enhance it further. However, if these variables are increased to speed up reaction, it makes sense to favor mass transfer as well (higher pressure and superficial gas velocities) to obtain the desired performance. Differently, if the mass transfer is not increased the same way as kinetics, then, a temperature or/and catalyst increase may not have the desired effect on conversion.

A similar analysis was performed for trickle bed reactors. Pressure and temperature influence were also studied for hydrogenation purposes. Furthermore, gas and liquid flowrates have an impact on conversion. Thus, trickle bed hydrogenation conversion for 1,2-dimethylindole and 7-ethylindole system is included in Figure 6 to analyze their effects. However, in this case, the trickle bed reactor feed was chosen not to be pure. This is because they tend to work for low reactant concentrations regarding to Roininen et al. (2009). Otherwise, the catalyst may be damaged at high temperatures due to the exothermal hydrogenation. A maximum temperature increase of 30 K over the trickle bed is considered as the upper limit (Satterfield, 1975). Thus, to meet these requerients, reactant concentrations in the liquid phase ranging 5-10% are selected to feed the trickle bed reactor. Strategies such as stream recycling or using a slurry-trickle combination can be proposed. This configuration can be found for similar hydrogenation systems as benzene (Zehner and Kraume, 2000).

Temperature and pressure have a positive impact on conversion as in the case of the slurry. They will favor hydrogen transference to the liquid phase. Hence, both will have

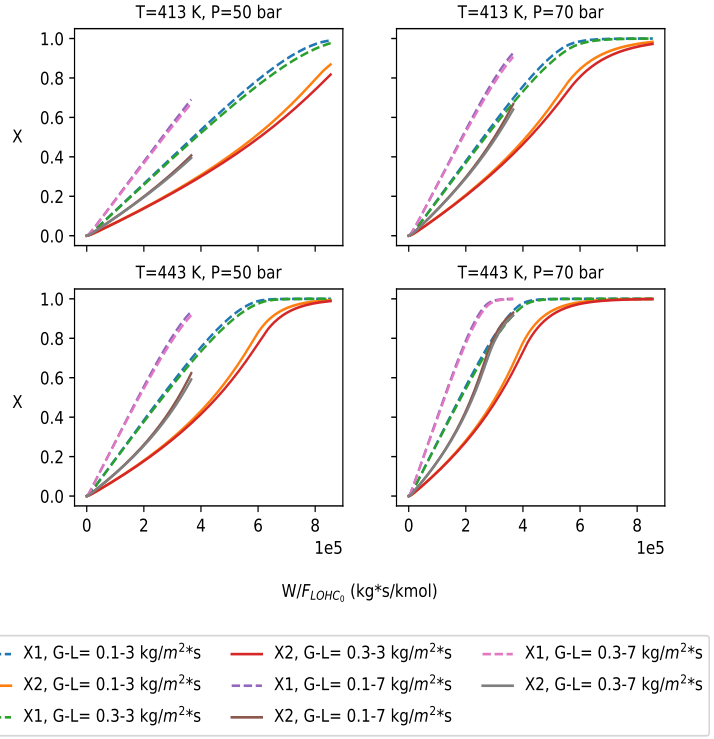

Figure 6: 1,2-dimethylindole (1) and 7-ethylindole (2) conversion in trickle bed reactor for different operating conditions. 9:1 molar relation perhydro-1,2-dimethylindole: 1,2-dimethylindole, 9:1 molar relation perhydro-7-ethylindole: 7-ethylindole, 1:1 molar relation perhydro-1,2-dimethylindole + 1,2-dimethylindole : perhydro-7-ethylindole + 7-ethylindole

great relevance in this reactor design as gas-liquid is clearly the main reaction resistance over the entire unit length (85-95%). The remaining contribution will be due to the liquid-to-particle resistance (3-4%) and kinetics (up to 10%). Only by the end of the reactor, when LOHCs concentration drops to lower levels, kinetic resistance experiments a sudden increase to values up to 80-90%, while liquid-to-particle still accounts for 10-20%. This alternancy of limiting stages is reflected in Figure 6 with a change of tendency in the last section of the reactor analyzed. Liquid and gas flowrates will have opposite effects on the conversion. On the one hand, as liquid feed increases, mass transfer coefficients are enhanced. Thus, better catalyst use and conversions are expected. On the other, for higher gas flowrates, although they favor mass and heat transfer, larger pressure drops are generated. It has a clear negative effect, especially at lower temperatures and pressures, in a reactor where hydrogen solubility plays a fundamental role. It must be noticed, however, that, reducing gas flowrates below the pulsing region is not recommended. It may cause a considerable reduction in mass transfer as a result.

Analogous behaviour is obtained for trickle bed dybenzyltoluene hydrogenation reactor: a large gas-liquid controlling region (65-95%) is found in the first stages to end with a second zone where kinetics will have larger importance (up to 95%). The remaining contribution at the end of the reactor is held by liquid-to-particle mass transfer (5-20%). In this case, from 1000 to 2000 kg_{cat}·s/mol will be required to reach complete conversions for dybenzyltoluene depending on the operating conditions. Around 0.4 K maximum temperature increase from catalyst to bulk media is found from both designs. This low temperature gradient is beneficial to avoid hot spots.

3.2. LOHCs dehydrogenation

The performance of dehydrogenation reactors is studied in this section. The fact that hydrogenation kinetics were faster than dehydrogenation ones made a large difference in reactor design. In the case of slurry dehydrogenation reactors, kinetics are far slower compared to liquid-to-particle mass transfer. It makes temperature and catalyst concentration to be the most relevant parameters. As a result, an increase in catalyst concentration and higher temperatures were required compared to hydrogenation reactors to avoid larger unit sizes. The influence of both variables on the conversion is shown in Figure 7 for the slurry dybenzyltoluene dehydrogenation reactor. For the other LOHCs studied system, 1,2-dimethylindole and 7-ethylindole, similar behaviour is found. Nevertheless, the system faster kinetics make possible to reach higher conversions at lower normalized volumes and temperatures (443-473 K). Specifically, 50 m^3·s/kmol for 1,2-dimethylindole and 250 m^3·s/kmol for 7-ethylindole are required to reach 80% conversion at 473 K and 500 kg/m^3 catalyst concentration. Other variables such as gas superficial velocities do not have any or negligible impact on the reaction as it is largely kinetic controlled. However, although reaction development will not be directly affected, the superficial gas velocity will have a major effect in heat transfer, reactor hold-up, and catalyst handling. Similarly, reactor pressure will not be as crucial as for hydrogenation units, but it must be higher than the pressure drop.

Kinetics have a great importance in the trickle bed dehydrogenation reactor design. For that reason, catalyst mass and operating temperature will be relevant variables too. Although kinetics dominate the rate, the mass transfer can also be considerable, specially at the beginning of the reactor where temperatures are higher. In the indoles system the contribution of the mass transfer in some cases can be significant (up to 85% and 55% for 1,2-dimethylindole and 7-ethylindole respectively), whereas for the dybenzyltoluene system its influence is lower (20% as maximum).

The temperature dependence is an issue since the adiabatic operation causes a temperature drop over the reactor length. In order to control temperature reduction, similar concentrations as for trickle hydrogenation units are taken for the reactants (5-10%).

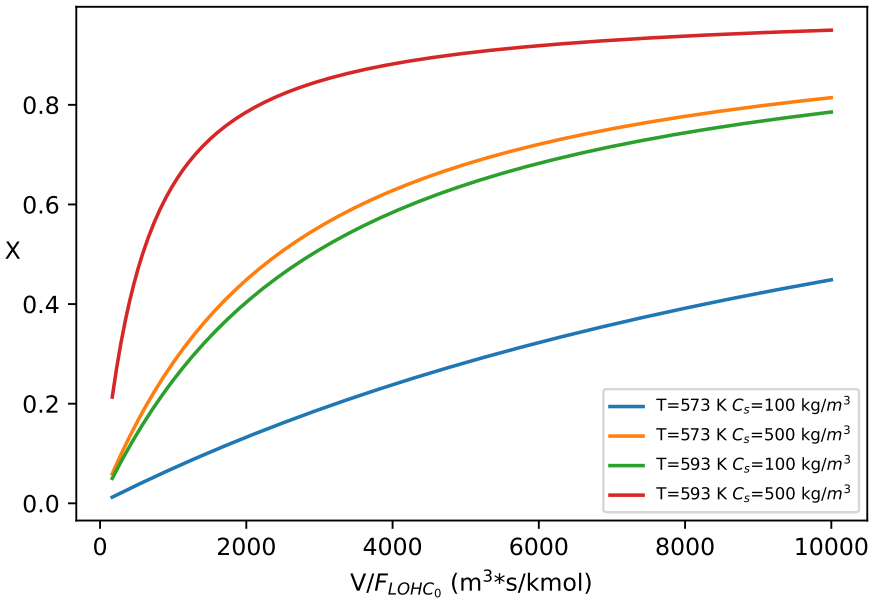

Figure 7: Perhydro-dibenzyltoluene dehydrogenation conversion (pure feed) in slurry reactor for different operating conditions

Then, a recycle stream or a series slurry-trickle reactor configurations are proposed to favor catalyst use. Furthermore, higher temperatures than hydrogenation ones are used as dehydrogenation reactions demand them for an effective reaction progress. The inlet pressure will be adjusted up to 6 bar. Higher pressures are not used to avoid hydrogen accumulation in the liquid phase. However, working at medium-low pressures represents a major drawback for these trickle bed reactors. This is because catalyst bed height cannot be increased to avoid pressure drops larger than the feed pressure.

In spite of the importance of the kinetics on the operation of this unit, other variables such as liquid and gas flowrates will have also a certain influence on dehydrogenation conversion for both LOHCs systems studied. This is not only due to mass and heat transfer from liquid-to-particle but also to better maintain the temperature over the reactor length. Although liquid flowrates enhance mass and heat transfer, reducing the temperature differences between particles and bulk media (which reaches a maximum value of 0.4 K in the cases studied), higher gas-liquid relation is able to mitigate bulk temperature drop over catalyst bed. This reactor behaviour is presented for 1,2-dimethylindole and 7-ethylindole dehydrogenation trickle bed reactor in Figure 8. At the beginning of the reaction, better heat transfer combined with higher mass transfer

coefficients favors conversions when liquid flowrates are higher. This trend ends as the temperature is reduced. Then, conversions will be favored for lower liquid flowrates as gas is able to better control the temperature. With regards to gas flowrate, higher values will improve heat transfer and reduce temperature drop. It will be then beneficial to operate at higher gas flowrates. However, higher pressure drops are produced in this situation limiting the bed height.

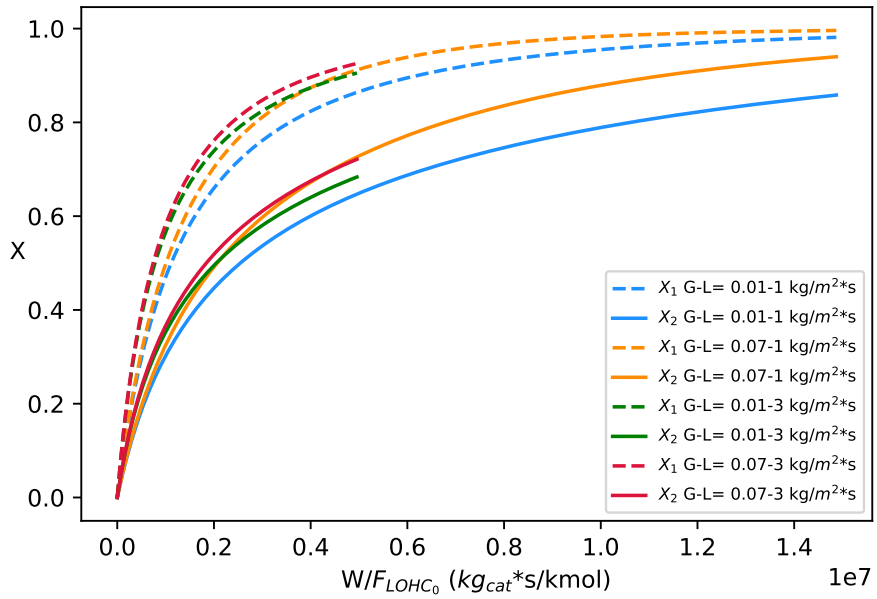

Figure 8: Perhydro-1,2-dimethylindole (1) and perhydro-7-ethylindole (2) dehydrogenation conversion in trickle bed reactor for different operating conditions. 1:9 molar relation perhydro-1,2-dimethylindole: 1,2-dimethylindole, 1:9 molar relation perhydro-7-ethylindole: 7-ethylindole, 1:1 molar relation perhydro-1,2-dimethylindole + 1,2-dimethylindole : perhydro-7-ethylindole + 7-ethylindole; T_{in}=473 K; P_{in}=5 bar

Higher catalyst mass is required for trickle bed reactors when dybenztyltoluene dehydrogenation is carried out. From 21000 to 27000 kg_{cat}·s/mol are required to reach 45% conversion for same inlet conditions as previous LOHCs system, althought inlet temperature was adjusted to 593 K. This occurs because of dybenzyltoluene system has lower kinetics and large dependence on temperature. It highly limits conversions because of reaction endothermicity to values up to 70%. It is not possible either to increase the reactor bed to fully dehydrogenate liquid as the pressure drop would be higher than the inlet pressure. In spite of these lower conversion results, similar behaviour is found compared to the previous system. First, liquid flowrates will favor conversion to end

up with a second phase where better results are expected at lower liquid flowrates. Furthermore, increasing gas flowrates will also lead to better results as temperature fall is minimized.

3.3. Surrogate models development

Once presented reactor models and analyzed the most relevant operating and design variables influence, a series of surrogate models were developed. The large number of variables and the presence of differential and high non-linear equations in the model makes difficult to implement the performance of these units at process scale formulations. Therefore, the development of simpler surrogate models based on a polynomial formulation with double interactions is proposed. Hence, this practice allows to obtain simple expressions enabling an easier implementation in process design. Thus, it would be possible to estimate unit performance easier. For that, the most representative operating and design parameters together with quadratic and interaction terms between them are included in these models based on AICc criteria (Hurvich and Tsai, 1989). The possible selected variables for surrogate models for both reactor designs are: operating pressure and temperature, unit diameter and reactives inlet. Moreover, gas and liquid flowrates, catalyst weight, and normalized catalyst weight can be also included for trickle bed designs, whereas, superficial gas velocity, catalyst concentration, reactor volume and normalized volume for slurry reactors. The surrogate models obtained for each reactor are included in the Supplementary Material.

Then, the proposed models are implemented in a General Algebraic Modeling System (GAMS) NLP formulation to determine the optimal values for the two proposed objective functions considering an isolated reactor unit. These are: reactor investment cost and catalyst usage. The reactor cost is estimated from the sum of the catalyst cost (500\$/kg$_{cat}$) (Dutta, 2016), the cost of the vessel and in the case of slurry reactors also the cost of heat exchange tubes. Sinnott and Towler (2020b) expressions are used to account for the cost of the vessel and the internal tubes. Several design constraints described in previous sections are also to be included (aspect ratios, heat exchange phenomena, pressure drop, mass and energy balances ...) and maximum and minimum limits for operating (gas flowrates, temperature, pressure, ...) and design variables (diameter, catalyst, length,...) are set. Final conversion results for slurry and trickle bed reactors and their relative errors (between brackets referred to the original model) are included in Tables 4 and 5 for both optimized functions. Results obtained show a good agreement between both models since an average error of 8.56% is found for these cases. They will be then useful to perform rough estimates for the performance of these reactors. The specific design and operating variables for each reactor are shown in the Table 6 and Table 7 for trickle bed and slurry respectively.

Table 4: Conversion results for reactor costs optimization

	Hydrogenation				Dehydrogenation			
	Slurry DBT	Slurry INDOL	Trickle DBT	Trickle INDOL	Slurry DBT	Slurry INDOL	Trickle DBT	Trickle INDOL
X_{DBT} or $X_{1,2-DMI}$	0.643 (4.17%)	0.913 (1.00%)	0.523 (1.45%)	1.000 (0.60%)	0.643 (9.18%)	0.822 (11.04%)	0.237 (2.86%)	0.621 (15.51%)
X_{7-EI}	-	0.553 (3.32%)	-	0.630 (23.41%)	-	0.624 (16.91%)	-	0.417 (13.93%)

Table 5: Conversion results for catalyst use optimization

	Hydrogenation				Dehydrogenation			
	Slurry DBT	Slurry INDOL	Trickle DBT	Trickle INDOL	Slurry DBT	Slurry INDOL	Trickle DBT	Trickle INDOL
X_{DBT} or $X_{1,2-DMI}$	0.643 (2.28%)	0.912 (1.79%)	0.523 (1.45%)	1.000 (0.60%)	0.643 (9.18%)	0.822 (11.04%)	0.237 (2.86%)	0.621 (15.51%)
X_{7-EI}	-	0.534 (3.09%)	-	0.630 (23.41%)	-	0.624 (16.91%)	-	0.417 (13.93%)

Table 6: Trickle bed optimized designs for the proposed optimization functions

	DBT hydrogenation		INDOL hydrogenation		DBT dehydrogenation		INDOL dehydrogenation	
	Costs	Catalyst use	Costs	Catalyst use	Costs	Catalyst use	Costs	Catalyst use
L_{in}/G_{in}	37.04	37.04	33.33	33.33	50.00	50.00	166.67	166.67
T_{in} (K)	413.00	413.00	443.00	443.00	593.00	593.00	473.00	473.00
W (kg_{cat})	971.35	971.35	317.74	317.74	5951.74	5951.74	2411.16	2411.16
P (bar)	70.00	70.00	53.54	53.54	5.38	5.38	2.47	2.47
D_T (m)	0.91	0.91	0.60	0.60	1.38	1.38	1.02	1.02
$L_{reactor}$ (m)	1.54	1.54	1.15	1.15	4.13	4.13	3.05	3.05
cost ($)	0.59	0.59	0.21	0.21	3.04	3.04	1.24	1.24

Slurry reactors design was optimized for a 30 ton_{H_2}/d hydrogenation/dehydrogenation capacity regarding similar energy storage capacity proposed for mid-scale transportation purposes acording to Weichenhain (2021).

Slurry designs were restricted to have minimum and maximum aspect ratios of 4 and 20 respectively regarding previous typical industrial values (Behkish et al., 2006). Moreover, minimum 0.08 m/s superficial gas velocity is adjusted to perform the design. Medium-high conversions are obtained for slurry reactor designs as expected, avoiding full hydrogenation/dehydrogenation of LOHCs. Some operating variables as temperature and superficial gas velocities reach the upper limits for the proposed range in hydrogenation reactors. The first one is because hydrogen solubility and reaction kinetics are favored. With regards to gas velocity, it is maximized due to a better mass transfer. Other variables such as pressure experiment changes from two proposed objective functions. Minimun and maximun levels are set for cost and catalyst usage minimization respectively. On the one hand, higher pressure favors more efficient catalyst use, on the other, it affects directly vessel cost. For the dehydrogenation reactors, the temperature is assigned to the highest value due to its kinetic favoring. With regards to the superficial gas velocities, lower values than the upper limits are established. They avoid higher hold-up values whereas not unfavor heat transfer.

Finally, referring to reactor investment costs, results for hydrogenation slurry re-

Table 7: Slurry optimized designs for the proposed optimization functions

	DBT hydrogenation		INDOL hydrogenation		DBT dehydrogenation		INDOL dehydrogenation	
	Costs	Catalyst use	Costs	Catalyst use	Costs	Catalyst use	Costs	Catalyst use
T (K)	443.00	443.00	443.00	442.68	593.00	593.00	473.00	473.00
C_s (kg/m^3)	217.30	174.67	50.00	50.00	158.81	157.32	100.00	100.00
$u_{g,in}$ (m/s)	0.56	0.56	0.56	0.56	0.55	1.08	1.98	2.35
V_{sl} (m^3)	3.01	3.51	2.00	1.65	127.38	128.57	28.92	28.86
P (bar)	50.00	70.00	50.00	70.00	2.42	4.90	2.00	2.00
D_T (m)	1.00	1.20	1.00	1.00	3.17	3.64	2.50	2.59
$L_{reactor}$ (m)	5.49	4.78	4.00	4.00	19.80	16.87	10.00	10.35
cost (MM$)	0.59	0.69	0.27	0.33	10.57	10.88	1.61	1.78

actors, range from 0.78 to 1.99 M$ $\cdot$ s/kg_{H_2} whereas in the case of dehydrogenation 4.63-31.33 M$ $\cdot$ s/kg_{H_2} costs are expected. Hence, it can be seen clearly that dehydrogenation units are more expensive than hydrogenation ones, mainly as higher catalyst use is required.

Trickle bed reactors are not able to reach slurry reactors capacities. This is caused as considerable oversizing would be produced, but also because for higher loads, aspect ratios are considerably lower compared to typical values. Because of that, trickle bed design might be derived to lower production applications. For that reason, the same optimization as for slurry reactors was carried out for 1 ton_{H_2}/d hydrogenation and dehydrogenation capacity in trickle bed reactors. The selected capacity is near the range from Roininen et al. (2009), where a hydrogenation load between 3.2-3.7 ton_{H_2}/d is found for a benzene hydrogenation trickle bed.

For trickle design, liquid flowrates are assigned to the maximum allowable values in all cases as higher mass transfer coefficients are expected. In the case of gas flowrates, they are set to higher values for hydrogenation to avoid excessive temperature increase over bed length in spite of its higher pressure drop. For the same reason, in the dybenzyltoluene dehydrogenation unit, the maximum gas flowrate value is placed. It results in better temperature control, impacting this way positively on reaction progress. For the dehydrogenation of the indoles system however, an intermediate value was set. Higher gas flowrates were not required as a lesser dependence of kinetics with temperature exists. At the same time, pressure drop was minimized.

Finally, it is significant how designs tend to be equal from both objective functions optimization. This is caused by the higher catalyst use requirements of these reactors that are clearly the main cost contributor. Furthermore, it seems clear that trickle bed reactors are considerably more expensive for hydrogenation (18.14-50.98 M$ $\cdot$ s/kg_{H_2}) and dehydrogenation (107.14-262.66 M$ $\cdot$ s/kg_{H_2}) compared to previous slurry design. Likewise for slurry reactors, dehydrogenation units are also more expensive than hy-

drogenation ones.

4. Conclusions

A LOHCs reactor assessment is performed with the two most extended three-phase reactors (trickle bed and slurry). This work formulated a 1-dimension reactor model including mass, heat and momentum transfer along with kinetic. For that, the main operating and design variables influence was studied and each design characteristic regions were described.

In the slurry hydrogenation reactors, two operating behaviours are identified: a fully kinetic-controlled unit or a reactor divided into two zones (mass and kinetically controlled). The reactor will operate in one or the other depending essentially on catalyst load and operating conditions. With regards to the last operation mode, gas-liquid shows a relevant weight (60-95%) at lower reactor volumes. Hereinafter, it ends in a second one where kinetics becomes the controlling step. This change is reached up to 70% conversions for dybenzyltoluene and 70-95% and 40-70% for 1,2-dimethylindole and 7-ethylindole respectively. The pressure and superficial gas velocity seem beneficial to the mass-controlling zone. The temperature will be also beneficial, but has a higher impact on kinetics. Only at the end, a third operating regime may be found. It appears at higher LOHCs conversions and is characterized by having negligible gas-liquid resistance. Either the reactor is only kinetic or mass and kinetic controlled, two tendencies are found. A better performance is expected for the first one. In contrast, only one region appears for the trickle bed design. This unit is almost fully gas-liquid transfer controlled although, at the end, an abrupt change of tendency is produced due to an increase in kinetic resistance. Temperature and pressure will also favor conversion with other variables as liquid flowrates. However, gas flowrate will cause a higher pressure drop althought it was discovered as useful to control temperature. Once evaluated both designs, a worse catalyst use is found for trickle beds compared to slurries.

Related to dehydrogenation units, higher sizes are found compared to hydrogenation reactors. Kinetics is presented as the most relevant contributor in slurries. Notwithstanding, in trickle beds, mass transfer weight can be also relevant. In both designs, a great influence of temperature and catalyst exists. However, other variables such as superficial gas velocity in the slurry reactor and gas and liquid flowrates in trickle beds were also relevant. The intrinsic endothermicity of dehydrogenation was presented as a bottleneck of this reaction. On the one hand, slurry reactor structure allows for an isothermal operation. On the other hand, the reduction in the temperature over the trickle bed slows the reaction and, for instance, in dybenzyltoluene system, conversions

were limited (up to 70%). Similar to hydrogenation reactors, it can be appreciated a more efficient catalyst use in the slurry compared to trickle bed.

Finally, a series of surrogate models were developed for all reactor designs. These models are useful for process design and optimization. Then, the optimization of reactor costs and catalyst use was done. Some variations were discovered for slurry designs between both optimizations. Contrary, trickle bed designs tend to be equal. In general, the most favorable variables were set to their maximum values, while decreasing those which negatively affected. Furthermore, higher costs are shown for trickle bed reactors compared to slurry and from dehydrogenation to hydrogenation units.

Nomenclature

Variables and parameters

1,2-DMI	1,2-dimethylindole
7-EI	7-ethylindole
A	Heat transfer area (m^2)
a_m	Specific bed area (m^{-1})
C	Concentration ($kmol/m^3$)
Cp	Heat capacity ($kJ/kg \cdot K$)
C_s	Slurry catalyst concentration (kg_{cat}/m^3)
$C_{s,v}$	Slurry catalyst volume fraction (m^3_{cat}/m^3)
D	Diffusion coefficient (m^2/s)
DBT	Dibenzyltoluene
D_{eff}	Effective diffusion coefficient (m^2/s)
d_h	Hydraulic diameter (m)
d_o	Gas sparger hole diameter (m)
d_p	Particle diameter (m)
d_{Sauter}	Bubble Sauter mean diameter (m)
D_T	Reactor diameter (m)
F	Molar flow (kmol/s)
Fr	Froude adimensional number
G	Gas flowrate ($kg/m^2 \cdot s$)
g	Gravity acceleration (m/s^2)
GHG	Greenhouse gas emissions
H	Henry coefficient
h_{l-s}	Liquid-to-particle convection heat transfer coefficient ($W/m^2 \cdot K$)
h_{sl}	Slurry convection heat transfer coefficient ($W/m^2 \cdot K$)

H_l	Slurry static liquid head (m)
ΔH_r	Reaction enthalpy (kJ/kmol)
k	Kinetic constant (s^{-1})
Kd	Gas sparger constant 1
$k_l a_g$	Gas-liquid mass transfer coefficient (s^{-1})
$k_m a_m$	Liquid-to-particle mass transfer coefficient (s^{-1})
L	Liquid flowrate ($kg/m^2 \cdot s$)
L_o	Distance between holes in gas sparger (m)
L_{pipe}	Pipe lenght (m)
$L_{reactor}$	Reactor lenght (m)
LOHC	Liquid Organic Hydrogen Carrier
MW	Molecular weight (kg/kmol)
n	Reaction order
n_l	Trickle bed gas-to-liquid mass transfer coefficient parameter 2
N_o	Gas sparger number of orifices
n_s	Trickle bed liquid-to-particle mass transfer coefficient parameter 2
ΔP_g	Gas independent bed pressure drop (Pa/m)
ΔP_l	Liquid independent trickle bed pressure drop (Pa/m)
ΔP_{lg}	Two-phase trickle bed pressure drop (Pa/m)
P	Pressure (bar)
pitch	Gas sparger hole pitch (m)
PH-1,2-DMI	Perhydro-1,2-dimethylindole
PH-7-EI	Perhydro-7-ethylindole
PHDBT	Perhydrodibenzyltoluene
Pr	Prandtl adimensional number
r	Reaction rate ($kmol/s \cdot m^3$)
Re	Reynolds adimensional number
ΔT	Slurry - heating/cooling agents temperature difference (K)
T_l	Trickle bed bulk temperature (K)
T_{sl}	Slurry temperature (K)
T_s	Surface temperature (K)
U	Overall heat transfer coefficient (W/m^2K)
u	Superficial velocity (m/s)
u′	Linear velocity (m/s)
u_{weep}	Weeping velocity for the gas sparger (m/s)
V	Reactor volume (m^3)
v	Stoichometric coefficient

V_g, SB	Small bubble rise velocity with solids (m/s)
V_g, SB_0	Small bubble rise velocity with no solids (m/s)
v_s	Slurry particles settling velocity (m/s)
W	Catalyst mass (kg)
We	Weber adimensional number
w_f	Wetting factor
X	Conversion
X_w	Main slurry component weight concentration
α_l	Trickle bed gas-to-liquid mass transfer coefficient parameter 1
α_s	Trickle bed liquid-to-particle mass transfer coefficient parameter 1
α_{gs}	Gas sparger constant 2
χ	Trickle bed pressure drop calculation coefficient
η	Catalyst effectiveness factor
ϵ	Bed porosity
ϵ_{in}	Catalyst internal porosity
$\epsilon_{dynamic}$	Dynamic external trickle bed hold-up
ϵ_g	Slurry reactor gas hold-up
$\epsilon_{g_{trans}}$	Transition gas hold-up with solids
$\epsilon_{g_{trans_0}}$	Transition gas hold-up with no solids
ϵ_{static}	Static external trickle bed hold-up
Γ	Gas sparger parameter
μ	Viscosity ($kg/m \cdot s$)
ϕ	Thiele Modulus
ρ	Density (kg/m^3)
σ	Surface tension (m/s)
τ	Tortuosity factor

Indexes

g	Gas phase
i	Component i
l	Liquid phase
s	Solid phase
sl	Slurry phase
jB	Bubble size j
SB	Small bubble
LB	Large bubble

Acknowledgments

This work was supported by the Regional Government of Castilla y León (Junta de Castilla y León) and by the Ministry of Science and Innovation MICIN and the European Union NextGenerationEU/PRTR (H2MetAmo project-C17.I01.P01.S21) and the FPU, Spain grant (FPU21/02413) to C.P.

References

Azarpour, A., Rezaei, N., Zendehboudi, S., 2021. Performance analysis and modeling of catalytic trickle-bed reactors: a comprehensive review. Journal of Industrial and Engineering Chemistry 103, 1–41. URL: https://www.sciencedirect.com/science/article/pii/S1226086X21002136, doi:https://doi.org/10.1016/j.jiec.2021.04.020.

Behkish, A., Lemoine, R., Oukaci, R., Morsi, B.I., 2006. Novel correlations for gas holdup in large-scale slurry bubble column reactors operating under elevated pressures and temperatures. Chemical Engineering Journal 115, 157–171. URL: https://www.sciencedirect.com/science/article/pii/S1385894705003633, doi:https://doi.org/10.1016/j.cej.2005.10.006.

Besagni, G., Gallazzini, L., Inzoli, F., 2019. On the scale-up criteria for bubble columns. Petroleum 5, 114–122. URL: https://www.sciencedirect.com/science/article/pii/S2405656117301645, doi:https://doi.org/10.1016/j.petlm.2017.12.005.

Bhaskar, M., Valavarasu, G., Sairam, B., Balaraman, K.S., Balu, K., 2004. Three-phase reactor model to simulate the performance of pilot-plant and industrial trickle-bed reactors sustaining hydrotreating reactions. Industrial & Engineering Chemistry Research 43, 6654–6669. URL: https://doi.org/10.1021/ie049642b, doi:10.1021/ie049642b, arXiv:https://doi.org/10.1021/ie049642b.

Biardi, G., Baldi, G., 1999. Three-phase catalytic reactors. Catalysis Today 52, 223–234. URL: https://www.sciencedirect.com/science/article/pii/S0920586199000772, doi:https://doi.org/10.1016/S0920-5861(99)00077-2.

BloombergNEF, 2021. New energy outlook 2021. URL: https://about.bnef.com/new-energy-outlook/.

Boelhouwer, J., Piepers, H., Drinkenburg, A., 2001. Particle–liquid heat transfer in trickle-bed reactors. Chemical Engineering Science 56, 1181–1187. URL: https://www.sciencedirect.com/science/article/pii/S0009250900003389, doi:https://doi.org/10.1016/S0009-2509(00)00338-9. 16th International Conference on Chemical Reactor Engineering.

Buwa, V.V., Roy, S., Ranade, V.V., 2016. Three-phase slurry reactors. John Wiley and Sons, Ltd. chapter 6. pp. 132–155. URL: https://onlinelibrary.wiley.com/doi/abs/10.1002/9781119248491.ch6, doi:https://doi.org/10.1002/9781119248491.ch6, arXiv:https://onlinelibrary.wiley.com/doi/pdf/10.1002/9781119248491.ch6.

Byun, M., Lee, A., Cheon, S., Kim, H., Lim, H., 2022. Preliminary feasibility study for hydrogen storage using several promising liquid organic hydrogen carriers: Technical, economic, and environmental perspectives. Energy Conversion and Management 268, 116001. URL: https://www.sciencedirect.com/science/article/pii/S0196890422007944, doi:https://doi.org/10.1016/j.enconman.2022.116001.

Capurso, T., Stefanizzi, M., Torresi, M., Camporeale, S., 2022. Perspective of the role of hydrogen in the 21st century energy transition. Energy Conversion and Management 251, 114898. URL: https://www.sciencedirect.com/science/article/pii/S0196890421010748, doi:https://doi.org/10.1016/j.enconman.2021.114898.

Chen, Z., Yang, M., Zhu, T., Zhang, Z., Chen, X., Liu, Z., Dong, Y., Cheng, G., Cheng, H., 2018. 7-ethylindole: A new efficient liquid organic hydrogen carrier with fast kinetics. International Journal of Hydrogen Energy 43, 12688–12696. URL: https://www.sciencedirect.com/science/article/pii/S0360319918308498, doi:https://doi.org/10.1016/j.ijhydene.2018.03.088. china-Europe Forum for Advanced Fuel Cell and New Energy.

Colbertaldo, P., Agustin, S.B., Campanari, S., Brouwer, J., 2019. Impact of hydrogen energy storage on california electric power system: Towards 100% renewable electricity. International Journal of Hydrogen Energy 44, 9558–9576. URL: https://www.sciencedirect.com/science/article/pii/S0360319918336449, doi:https://doi.org/10.1016/j.ijhydene.2018.11.062.

Dong, Y., Yang, M., Li, L., Zhu, T., Chen, X., Cheng, H., 2019. Study on reversible hydrogen uptake and release of 1,2-dimethylindole as a new liquid organic hydrogen carrier. International Journal of Hydrogen Energy 44, 4919–4929. URL: https://www.sciencedirect.com/science/article/pii/S0360319919300588, doi:https://doi.org/10.1016/j.ijhydene.2019.01.015.

Dorostkar, E., Khademi, M.H., Rahimi, A., 2021. Modeling of slurry bubble-column reactors with emphasis on the importance of bubble size estimation. Chemical Engineering & Technology 44, 417–430. URL: https://onlinelibrary.wiley.com/doi/abs/10.1002/ceat.202000231, doi:https://doi.org/10.1002/ceat.202000231, arXiv:https://onlinelibrary.wiley.com/doi/pdf/10.1002/ceat.202000231.

Dutta, A., S.J.H.D.B.F.S.A., 2016. Conceptual process design and techno-economic assessment of ex situ catalytic fast pyrolysis of biomass: A fixed bed reactor implementation scenario for future feasibility. Topics in Catalysis 59, 2–18. doi:https://doi.org/10.1007/s11244-015-0500-z.

Ekambara, K., Dhotre, M.T., Joshi, J.B., 2005. Cfd simulations of bubble column reactors: 1d, 2d and 3d approach. Chemical Engineering Science 60, 6733–6746. URL: https://www.sciencedirect.com/science/article/pii/S0009250905004963, doi:https://doi.org/10.1016/j.ces.2005.05.047.

Ellman, M., Midoux, N., Wild, G., Laurent, A., Charpentier, J., 1990. A new, improved liquid hold-up correlation for trickle-bed reactors. Chemical Engineering Science 45, 1677–1684. URL: https://www.sciencedirect.com/science/article/pii/000925099087046U, doi:https://doi.org/10.1016/0009-2509(90)87046-U.

Ergun, S., 1952. Fluid flow through packed columns.

Eypasch, M., Schimpe, M., Kanwar, A., Hartmann, T., Herzog, S., Frank, T., Hamacher, T., 2017. Model-based techno-economic evaluation of an electricity storage system based on liquid organic hydrogen carriers. Applied Energy 185, 320–330. URL: https://www.sciencedirect.com/science/article/pii/S0306261916315094, doi:https://doi.org/10.1016/j.apenergy.2016.10.068.

Forret, A., Schweitzer, J.M., Gauthier, T.P., Krishna, R., Schweich, D., 2006. Scale up of slurry bubble reactors. Journal of Physical Chemistry A .

Goto, S., Smith, J.M., 1975. Trickle-bed reactor performance. part i. holdup and mass transfer effects. AIChE Journal 21, 706–713. URL: https://aiche.onlinelibrary.wiley.com/doi/abs/10.1002/aic.690210410, doi:https://doi.org/10.1002/aic.690210410.

Gür, T.M., 2018. Review of electrical energy storage technologies, materials and systems: challenges and prospects for large-scale grid storage. Energy Environ. Sci. 11, 2696–2767. URL: http://dx.doi.org/10.1039/C8EE01419A, doi:10.1039/C8EE01419A.

He, T., Pei, Q., Chen, P., 2015. Liquid organic hydrogen carriers. Journal of Energy Chemistry 24, 587–594. URL: https://www.sciencedirect.com/science/article/pii/S2095495615000546, doi:https://doi.org/10.1016/j.jechem.2015.08.007.

Hren, R., Vujanović, A., Van Fan, Y., Klemeš, J.J., Krajnc, D., Čuček, L., 2023. Hydrogen production, storage and transport for renewable energy and chemicals: An environmental footprint assessment. Renewable

and Sustainable Energy Reviews 173, 113113. URL: https://www.sciencedirect.com/science/article/pii/S1364032122009947, doi:https://doi.org/10.1016/j.rser.2022.113113.

Hurvich, C.M., Tsai, C.L., 1989. Regression and time series model selection in small samples. Biometrika 76, 297–307. URL: https://doi.org/10.1093/biomet/76.2.297, doi:10.1093/biomet/76.2.297.

Iliuta, I., Larachi, F., 2016. Three-phase fixed-bed reactors. John Wiley and Sons, Ltd. chapter 5. pp. 95–131. URL: https://onlinelibrary.wiley.com/doi/abs/10.1002/9781119248491.ch5, doi:https://doi.org/10.1002/9781119248491.ch5, arXiv:https://onlinelibrary.wiley.com/doi/pdf/10.1002/9781119248491.ch5.

IRENA, 2020. Global renewables outlook: Energy transformation 2050.

Jarullah, A.T., Mujtaba, I.M., Wood, A.S., 2012. Whole crude oil hydrotreating from small-scale laboratory pilot plant to large-scale trickle-bed reactor: Analysis of operational issues through modeling. Energy & Fuels 26, 629–641. URL: https://doi.org/10.1021/ef201406r, doi:10.1021/ef201406r, arXiv:https://doi.org/10.1021/ef201406r.

Jorschick, H., Preuster, P., Dürr, S., Seidel, A., Müller, K., Bösmann, A., Wasserscheid, P., 2017. Hydrogen storage using a hot pressure swing reactor. Energy Environ. Sci. 10, 1652–1659. URL: http://dx.doi.org/10.1039/C7EE00476A, doi:10.1039/C7EE00476A.

Kenney, C., Sedriks, W., 1972. Effectiveness factors in a three-phase slurry reactor: the reduction of crotonaldehyde over a palladium catalyst. Chemical Engineering Science 27, 2029–2040. URL: https://www.sciencedirect.com/science/article/pii/0009250972870611, doi:https://doi.org/10.1016/0009-2509(72)87061-1.

Knobloch, F., Hanssen, S.V., Lam, A., Pollitt, H., Salas, P., Chewpreecha, U., Huijbregts, M.A., Mercure, J.F., 2020. Net emission reductions from electric cars and heat pumps in 59 world regions over time. Nature Sustainability 3, 437–447. doi:https://doi.org/10.1038/s41893-020-0488-7.

Krishna, R., Ellenberger, J., 1996. Gas holdup in bubble column reactors operating in the churn-turbulent flow regime. AIChE Journal 42, 2627–2634. URL: https://aiche.onlinelibrary.wiley.com/doi/abs/10.1002/aic.690420923, doi:https://doi.org/10.1002/aic.690420923.

Kulkarni, A.V., Joshi, J.B., 2011. Design and selection of sparger for bubble column reactor. part i: Performance of different spargers. Chemical Engineering Research and Design 89, 1972–1985. URL: https://www.sciencedirect.com/science/article/pii/S0263876211000128, doi:https://doi.org/10.1016/j.cherd.2011.01.004.

Kwak, Y., Kirk, J., Moon, S., Ohm, T., Lee, Y.J., Jang, M., Park, L.H., il Ahn, C., Jeong, H., Sohn, H., Nam, S.W., Yoon, C.W., Jo, Y.S., Kim, Y., 2021. Hydrogen production from homocyclic liquid organic hydrogen carriers (lohcs): Benchmarking studies and energy-economic analyses. Energy Conversion and Management 239, 114124. URL: https://www.sciencedirect.com/science/article/pii/S0196890421003009, doi:https://doi.org/10.1016/j.enconman.2021.114124.

Lemoine, R., Behkish, A., Sehabiague, L., Heintz, Y.J., Oukaci, R., Morsi, B.I., 2008. An algorithm for predicting the hydrodynamic and mass transfer parameters in bubble column and slurry bubble column reactors. Fuel Processing Technology 89, 322–343. URL: https://www.sciencedirect.com/science/article/pii/S0378382007002342, doi:https://doi.org/10.1016/j.fuproc.2007.11.016. special Issue in Honor of Professor Masakatsu Nomura.

Mamabolo, B.A., Nkazi, D., 2019. Modeling of a slurry bubble column reactor using a two-phase two-bubble class approach—a hydrodynamics study. Energy & Fuels 33, 612–628. URL: https://doi.org/10.1021/acs.energyfuels.8b02937, doi:10.1021/acs.energyfuels.8b02937.

Manjrekar, O.N., Mills, P.L., 2022. Trickle Bed Reactors. John Wiley and Sons, Ltd. chapter 9. pp. 533–588. URL: https://onlinelibrary.wiley.com/doi/abs/10.1002/9783527812066.ch9, doi:https://doi.org/10.1002/9783527812066.ch9, arXiv:https://onlinelibrary.wiley.com/doi/pdf/10.1002/9783527812066.ch9.

Maretto, C., Krishna, R., 1999. Modelling of a bubble column slurry reactor for fischer–tropsch synthesis. Catalysis Today 52, 279–289. URL: https://www.sciencedirect.com/science/article/pii/S0920586199000826, doi:https://doi.org/10.1016/S0920-5861(99)00082-6.

Meckling, J., Sterner, T., Wagner, G., 2017. Policy sequencing toward decarbonization. Nature Energy 2, 918–922. doi:https://doi.org/10.1038/s41560-017-0025-8.

Mederos, F.S., Ancheyta, J., Chen, J., 2009. Review on criteria to ensure ideal behaviors in trickle-bed reactors. Applied Catalysis A: General 355, 1–19. URL: https://www.sciencedirect.com/science/article/pii/S0926860X08007059, doi:https://doi.org/10.1016/j.apcata.2008.11.018.

Mederos-Nieto, F.S., Elizalde-Martínez, I., Trejo-Zárraga, F., Hernández-Altamirano, R., Alonso-Martínez, F., 2020. Dynamic modeling and simulation of three-phase reactors for hydrocracking of vegetable oils. Reaction Kinetics, Mechanisms and Catalysis 131, 613–644.

Mills, P.L., Dudukovic, M.P., 1981. Evaluation of liquid-solid contacting in trickle-bed reactors by tracer methods. AIChE Journal 27, 893–904. URL: https://aiche.onlinelibrary.wiley.com/doi/abs/10.1002/aic.690270604, doi:https://doi.org/10.1002/aic.690270604, arXiv:https://aiche.onlinelibrary.wiley.com/doi/pdf/10.1002/aic.690270604.

Modisha, P., Gqogqa, P., Garidzirai, R., Ouma, C.N., Bessarabov, D., 2019. Evaluation of catalyst activity for release of hydrogen from liquid organic hydrogen carriers. International Journal of Hydrogen Energy 44, 21926–21935. URL: https://www.sciencedirect.com/science/article/pii/S0360319919325182, doi:https://doi.org/10.1016/j.ijhydene.2019.06.212.

Narayanan, T.M., He, G., Gençer, E., Shao-Horn, Y., Mallapragada, D.S., 2022. Role of liquid hydrogen carriers in deeply decarbonized energy systems. ACS Sustainable Chemistry & Engineering 10, 10768–10780. URL: https://doi.org/10.1021/acssuschemeng.2c00909, doi:10.1021/acssuschemeng.2c00909, arXiv:https://doi.org/10.1021/acssuschemeng.2c00909.

Niermann, M., Drünert, S., Kaltschmitt, M., Bonhoff, K., 2019. Liquid organic hydrogen carriers (lohcs) – techno-economic analysis of lohcs in a defined process chain. Energy Environ. Sci. 12, 290–307. URL: http://dx.doi.org/10.1039/C8EE02700E, doi:10.1039/C8EE02700E.

Niermann, M., Timmerberg, S., Drünert, S., Kaltschmitt, M., 2021. Liquid organic hydrogen carriers and alternatives for international transport of renewable hydrogen. Renewable and Sustainable Energy Reviews 135, 110171. URL: https://www.sciencedirect.com/science/article/pii/S1364032120304627, doi:https://doi.org/10.1016/j.rser.2020.110171.

Preuster, P., Papp, C., Wasserscheid, P., 2017. Liquid organic hydrogen carriers (lohcs): Toward a hydrogen-free hydrogen economy. Accounts of Chemical Research 50, 74–85. URL: https://doi.org/10.1021/acs.accounts.6b00474, doi:10.1021/acs.accounts.6b00474, arXiv:https://doi.org/10.1021/acs.accounts.6b00474. pMID: 28004916.

Ramachandran, P., Chaudhari, R., 1983. Three-phase Catalytic Reactors. Studies in Cybernetics, Gordon and Breach Science Publishers.

Rao, P.C., Yoon, M., 2020. Potential liquid-organic hydrogen carrier (lohc) systems: A review on recent progress. Energies 13. URL: https://www.mdpi.com/1996-1073/13/22/6040, doi:10.3390/en13226040.

Reilly, I.G., Scott, D.S., Debruijn, T.J., Macintyre, D., 1994. The role of gas phase momentum in determining gas holdup and hydrodynamic flow regimes in bubble column operations. The Canadian Journal of Chemical Engineering 72, 3–12. URL: https://onlinelibrary.wiley.com/doi/abs/10.1002/cjce.5450720102, doi:https://doi.org/10.1002/cjce.5450720102, arXiv:https://onlinelibrary.wiley.com/doi/pdf/10.1002/cjce.5450720102.

Ritchie, H., Roser, M., Rosado, P., 2020. Co2 and greenhouse gas emissions. Our World in Data Https://ourworldindata.org/co2-and-other-greenhouse-gas-emissions.

Roininen, J., Alopaeus, V., Toppinen, S., Aittamaa, J., 2009. Modeling and simulation of an industrial trickle-

bed reactor for benzene hydrogenation: Model validation against plant data. Industrial & Engineering Chemistry Research 48, 1866–1872. URL: https://doi.org/10.1021/ie801411n, doi:10.1021/ie801411n.

Ross, J.R., 2019. Chapter 8 - mass and heat transfer limitations and other aspects of the use of large-scale catalytic reactors, in: Ross, J.R. (Ed.), Contemporary Catalysis. Elsevier, Amsterdam, pp. 187–213. URL: https://www.sciencedirect.com/science/article/pii/B9780444634740000084, doi:https://doi.org/10.1016/B978-0-444-63474-0.00008-4.

Samimi, F., Ahmadi, A.R., Dehghani, O., Rahimpour, M.R., 2015. De approach in development of a detailed reaction network for liquid phase selective hydrogenation of methylacetylene and propadiene in a trickle bed reactor. Industrial & Engineering Chemistry Research 54, 117–129. URL: https://doi.org/10.1021/ie503600b, doi:10.1021/ie503600b, arXiv:https://doi.org/10.1021/ie503600b.

Satterfield, C.N., 1975. Trickle-bed reactors. AIChE Journal 21, 209–228.

Satterfield, C.N., Pelossof, A.A., Sherwood, T.K., 1969. Mass transfer limitations in a trickle-bed reactor. AIChE Journal 15, 226–234. URL: https://aiche.onlinelibrary.wiley.com/doi/abs/10.1002/aic.690150219, doi:https://doi.org/10.1002/aic.690150219.

Sehabiague, L., Lemoine, R., Behkish, A., Heintz, Y.J., Sanoja, M., Oukaci, R., Morsi, B.I., 2008. Modeling and optimization of a large-scale slurry bubble column reactor for producing 10,000bbl/day of fischer–tropsch liquid hydrocarbons. Journal of the Chinese Institute of Chemical Engineers 39, 169–179. URL: https://www.sciencedirect.com/science/article/pii/S0368165307001190, doi:https://doi.org/10.1016/j.jcice.2007.11.003. festschrift Issue In honor of Professor Shiao-Hung Chiang.

Serrano-Arévalo, T.I., Tovar-Facio, J., Ponce-Ortega, J.M., 2023. Optimal incorporation of intermittent renewable energy storage units and green hydrogen production in the electrical sector. Energies 16. URL: https://www.mdpi.com/1996-1073/16/6/2609, doi:10.3390/en16062609.

Shen, Y., Maamor, A., Abu-Dharieh, J., Thompson, J.M., Kalirai, B., Stitt, E.H., Rooney, D.W., 2014. Moving from batch to continuous operation for the liquid phase dehydrogenation of tetrahydrocarbazole. Organic Process Research & Development 18, 392–401. URL: https://doi.org/10.1021/op400217d, doi:10.1021/op400217d.

Shi, L., Zhou, Y., Qi, S., Smith, K.J., Tan, X., Yan, J., Yi, C., 2020. Pt catalysts supported on h2 and o2 plasma-treated al2o3 for hydrogenation and dehydrogenation of the liquid organic hydrogen carrier pair dibenzyltoluene and perhydrodibenzyltoluene. ACS Catalysis 10, 10661–10671. URL: https://doi.org/10.1021/acscatal.0c03091, doi:10.1021/acscatal.0c03091, arXiv:https://doi.org/10.1021/acscatal.0c03091.

Sinnott, R., Towler, G., 2020a. Chapter 12 - heat-transfer equipment, in: Sinnott, R., Towler, G. (Eds.), Chemical Engineering Design (Sixth Edition). sixth edition ed.. Butterworth-Heinemann. Chemical Engineering Series, pp. 773–927. URL: https://www.sciencedirect.com/science/article/pii/B9780081025994000126, doi:https://doi.org/10.1016/B978-0-08-102599-4.00012-6.

Sinnott, R., Towler, G., 2020b. Chapter 6 - costing and project evaluation, in: Sinnott, R., Towler, G. (Eds.), Chemical Engineering Design (Sixth Edition). sixth edition ed.. Butterworth-Heinemann. Chemical Engineering Series, pp. 275–369. URL: https://www.sciencedirect.com/science/article/pii/B9780081025994000060, doi:https://doi.org/10.1016/B978-0-08-102599-4.00006-0.

Sáez, A.E., Carbonell, R.G., 1985. hydrodynamic parameters for gas-liquid cocurrent flow in packed beds. AIChE Journal 31, 52–62. URL: https://aiche.onlinelibrary.wiley.com/doi/abs/10.1002/aic.690310105, doi:https://doi.org/10.1002/aic.690310105, arXiv:https://aiche.onlinelibrary.wiley.com/doi/pdf/10.1002/aic.690310105.

Sánchez, A., Zhang, Q., Martín, M., Vega, P., 2022. Towards a new renewable power system using energy storage: An economic and social analysis. Energy Conversion and Management 252,

115056. URL: https://www.sciencedirect.com/science/article/pii/S0196890421012322, doi:https://doi.org/10.1016/j.enconman.2021.115056.

Thomaßen, G., Kavvadias, K., Jiménez Navarro, J.P., 2021. The decarbonisation of the eu heating sector through electrification: A parametric analysis. Energy Policy 148, 111929. URL: https://www.sciencedirect.com/science/article/pii/S0301421520306406, doi:https://doi.org/10.1016/j.enpol.2020.111929.

Wan, C., An, Y., Chen, F., Cheng, D., Wu, F., Xu, G., 2013. Kinetics of n-ethylcarbazole hydrogenation over a supported ru catalyst for hydrogen storage. International Journal of Hydrogen Energy 38, 7065–7069. URL: https://www.sciencedirect.com/science/article/pii/S0360319913008719, doi:https://doi.org/10.1016/j.ijhydene.2013.04.022.

Wang, T., Wang, J., Jin, Y., 2007. Slurry reactors for gas-to-liquid processes: a review. Industrial & Engineering Chemistry Research 46, 5824–5847. URL: https://doi.org/10.1021/ie070330t, doi:10.1021/ie070330t.

Wang, Y., Chen, J., Larachi, F., 2013. Modelling and simulation of trickle-bed reactors using computational fluid dynamics: A state-of-the-art review. The Canadian Journal of Chemical Engineering 91, 136–180. URL: https://onlinelibrary.wiley.com/doi/abs/10.1002/cjce.20702, doi:https://doi.org/10.1002/cjce.20702, arXiv:https://onlinelibrary.wiley.com/doi/pdf/10.1002/cjce.20702.

Weichenhain, U., 2021. Hydrogen transportation: The key to unlocking the clean hydrogen economy. Technical Report. Roland Berger GMBH.

Westerterp, K.R., Wammes, W.J.A., 2000. Three-Phase Trickle-Bed Reactors. John Wiley and Sons, Ltd. URL: https://onlinelibrary.wiley.com/doi/abs/10.1002/14356007.b04_309, doi:https://doi.org/10.1002/14356007.b04_309.

Zehner, P., Kraume, M., 2000. Bubble Columns. John Wiley and Sons, Ltd. URL: https://onlinelibrary.wiley.com/doi/abs/10.1002/14356007.b04_275, doi:https://doi.org/10.1002/14356007.b04_275.